# Characterization of Charge Spreading and Gain of Encapsulated Resistive Micromegas Detectors for HA-TPC of T2K


Samira Hassani, Jean-François Laporte

CEA-Saclay/DRF-IRFU, Univ. Paris – Saclay

on behalf of HA-TPC group


ICHEP, Prague, 18th - 24th July 2024

# Outline

1. Introduction of T2K Near Detector upgrade
2. Modeling of charge spreading with resistive Micromegas
3. Application of charge spreading model on X-ray data
4. Understanding the noise
5. Summary

# 1. Introduction

# The T2K experiment: Tokai to Kamioka

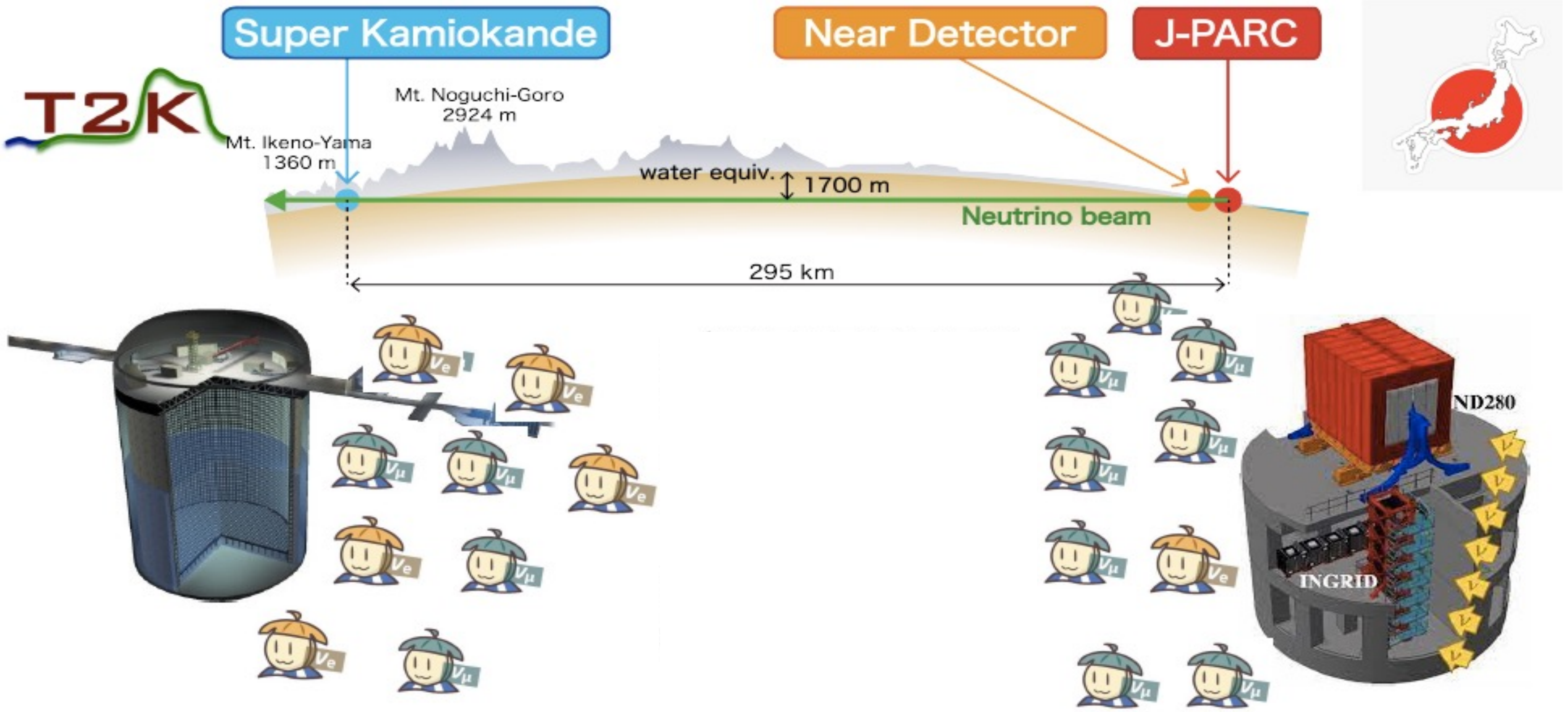


- **Main goals** :
  - Measure $\nu_e / \overline{\nu}_e$ appearance : sensitive to ($\theta_{13}$, $\delta_{CP}$)
  - Measure $\nu_\mu / \overline{\nu}_\mu$ disappearance : sensitive to ($\theta_{23}$, $\Delta m^2_{32}$)
- **First hint of CP violation in the lepton sector** : indication of maximal CP violation in neutrino oscillations $\delta_{CP} \sim -\pi/2$. *Nature 580, 339–344 (2020)*
- **The role of the Near Dector (ND280)** is to constrain the flux and cross-section systematics model by measuring neutrino interactions before the oscillations.
- T2K aims to determine CPV at the $3\sigma$ level in the coming years → Upgrade of ND280 and beam upgrade

# T2K Near Detector : ND280

*NIM A 659 (2011) 106–135, arXiv:1901.03750*

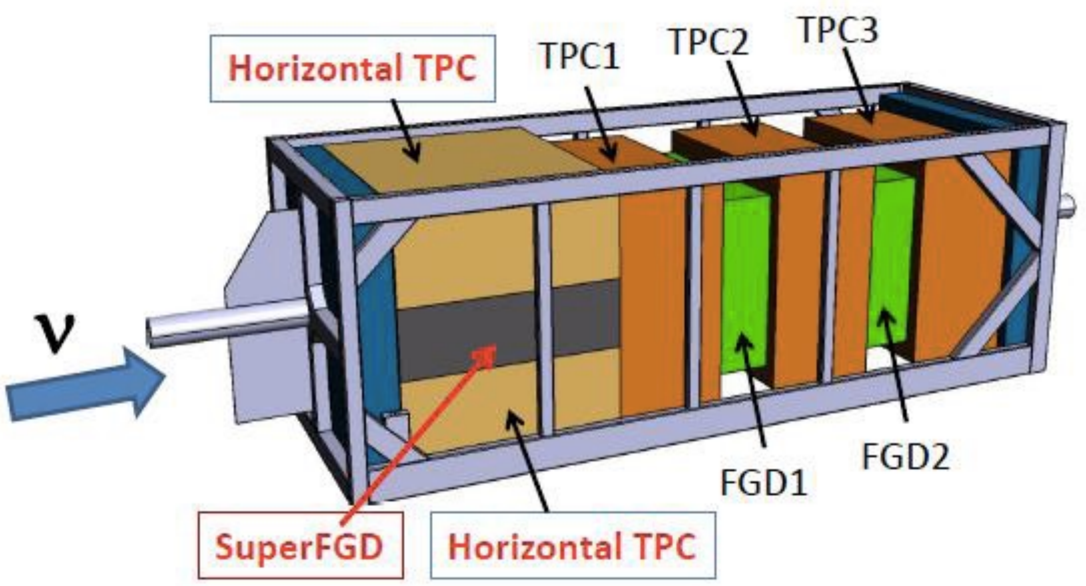


**New detectors**

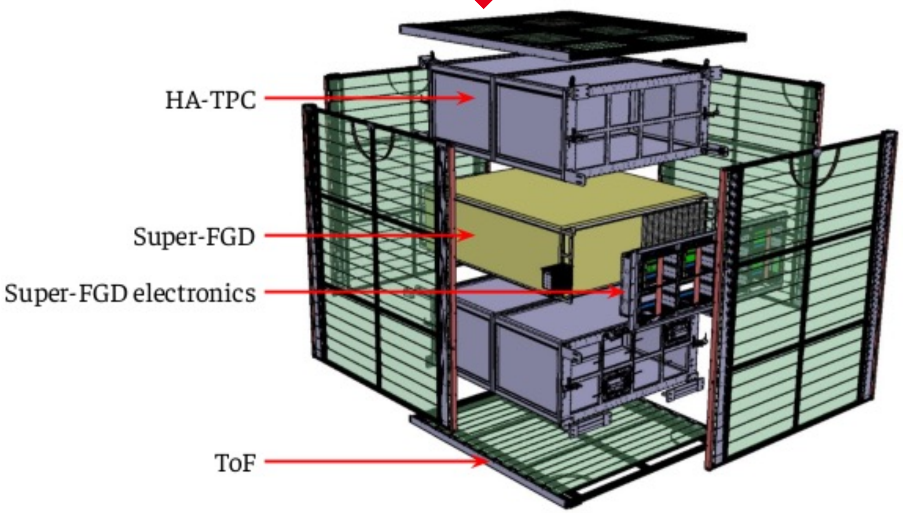


- Detector installed inside the UA1/NOMAD magnet (0.2 T)
- An electromagnetic calorimeter to distinguish tracks from showers
- A tracker system composed by:
  - Two Fine-Grain-Detectors (FGD) as neutrino active target
    - FGD1 (scintillator), FGD2 (scintillator: water)
- Three vertical Time Projection Chambers (TPC)

  **→ Readout using bulk MicroMegas**

- **New detectors to extend acceptance for tracks at high angles**
  - Super-FGD allow to fully reconstruct tracks in 3D → lower threshold and excellent resolution to reconstruct protons at any angle.

    →Neutrons will also be reconstructed via proton recoil.
  - Two High-Angle TPCs (HA-TPC) allow to reconstruct muons at any angle with respect to beam

    **→ Readout using resistive Micromegas**
  - ToF planes (x 6) allow to veto particles originating from outside the ND280 fiducial volume.

# ND280 Installation Completed in May 2024

top-HATPC

Super-FGD

bottom-HATPC

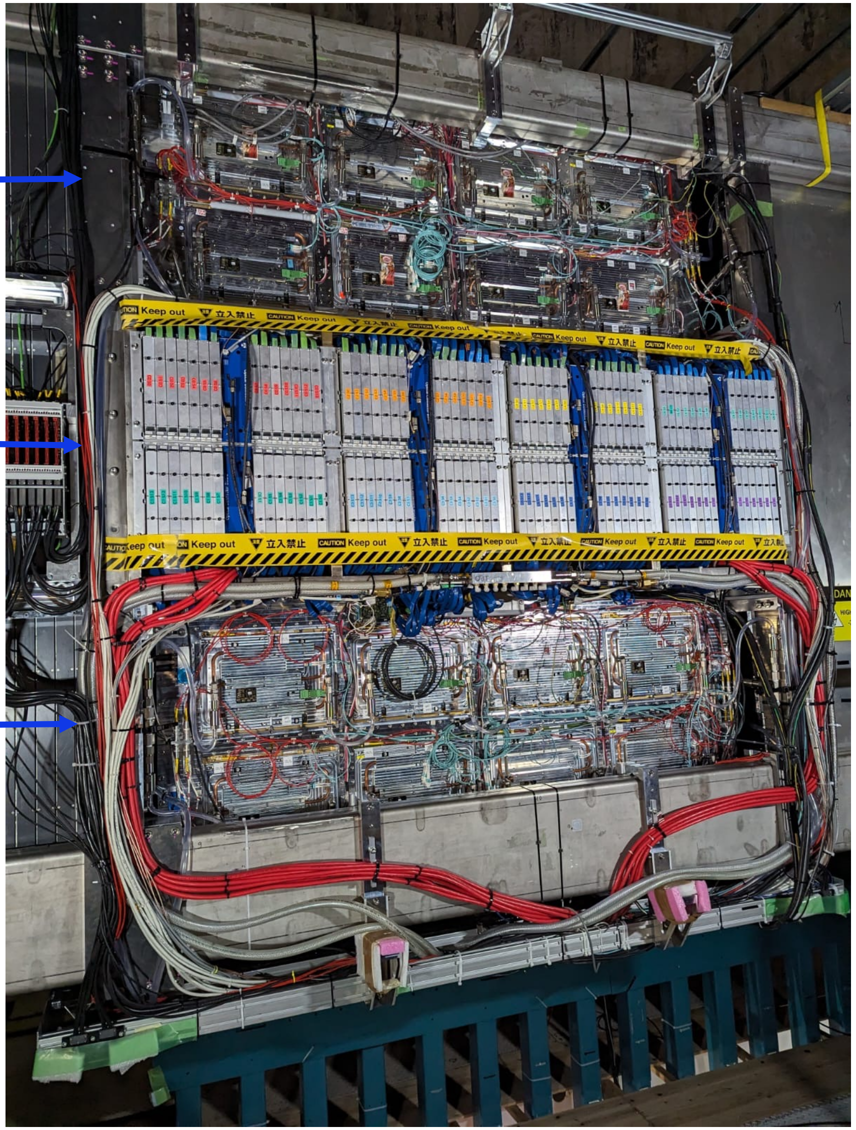

First neutrino interactions with full ND280 upgrade

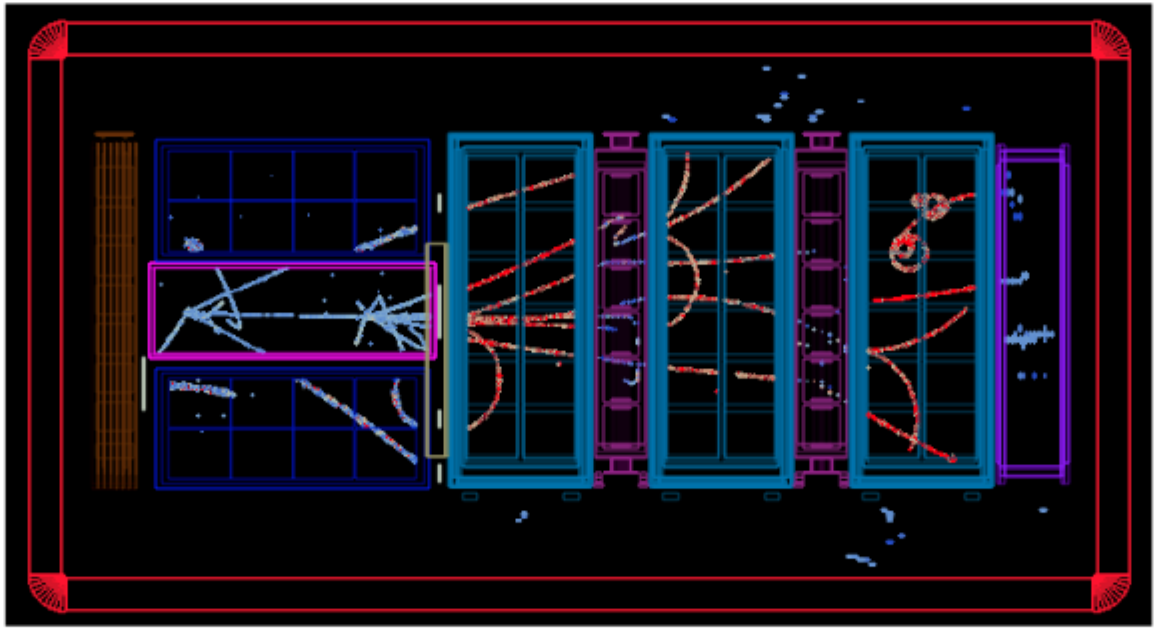

# High Angle TPC Specifications

- **Atmospheric pressure TPC**
  - Gas: T2K mixture (Ar-CF4-isoC4H10 = 95-3-2)
  - Gas contaminants better than O(10 ppm) level
  - Drift length 1m
  - Central Cathode @ -27kV
  - E field uniformity < $10^{-3}$ @1cm from walls
  - Low material budget, thin walls
  - Active volume ~ O($3m^3$)
- **Resistive MicroMegas sensors (ERAMs)**
  - Overall anode active surface ~ O(3 $m^2$)
  - Sampling length ~ 80-160 cm
  - pads ~ 1.1x1$cm^2$
  - 10k+10k channels / TPC @ End Plates (Anodes)

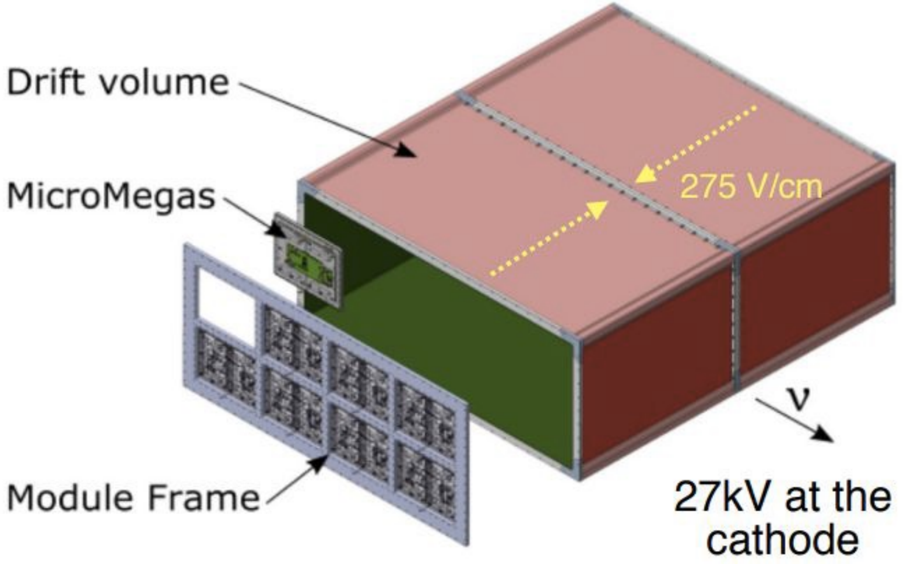


- Momentum resolution $\sigma_p/p$ < 10% at 1GeV/c (neutrino energy)
- Energy resolution $\sigma_{dE/dx}$ < 10% →(PID muons and electrons)
- Space resolution O(500 μm)→(3D tracking & pattern recognition)
- Low material budget walls ~ 3% $X_0$→(matching tracks from neutrino active target)

# Charge Readout – MicroMegas with Resistive Foil

- **Resistive layer enables charge spreading**
  - space resolution below 500 μm with cm size pads
  - less FEE channels (lower cost)
  - improved resolution at small drift distance (where transverse diffusion cannot help)
- **Resistive layer prevents sparks**
  - enables operation at higher gain
  - no need for spark protection circuits for ASICs → compact FEE → max active volume
- **Resistive layer encapsulated and properly insulated from Ground**
  - Mesh at ground and Resistive layer at +HV
  - improved field homogeneity → reduced track distortions

**Standard bulk-MicroMegas**

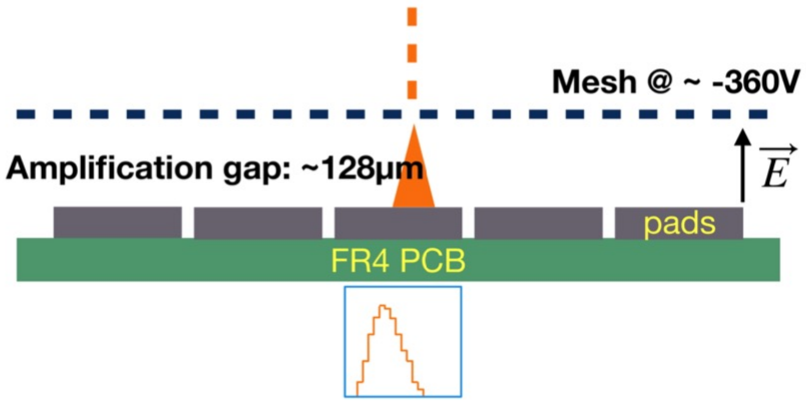


**Encapsulated Resistive Anode MicroMegas (ERAM)**

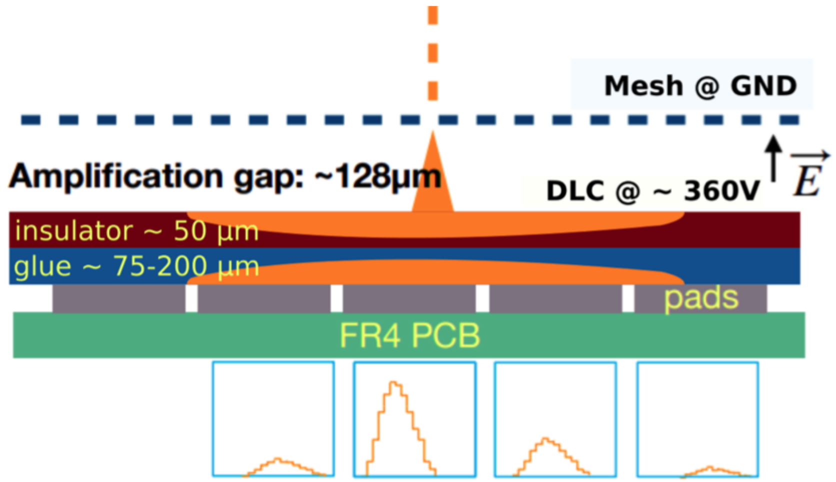

# Encapsulated Resistive Anode Micromegas (ERAM) Characteristics

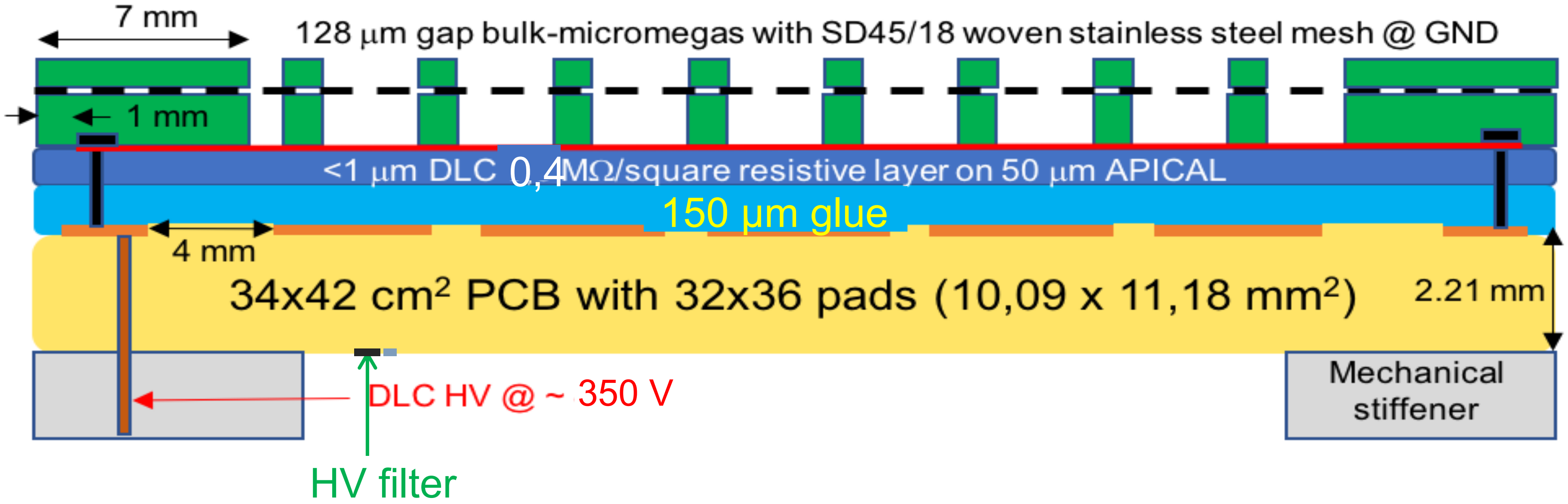


ERAMs very sensitive to dust

**Production version of the ERAM (Encapsulated Resistive Anode Micromegas) detector**

- Readout PCB: HA-TPC
- 36 × 32 pads
- 11,18 × 10,09 cm² pads
- ~400 kΩ/❑ (after annealing in air at 220°C, ~ 1MΩ/❑ before)
- 150 µm of glue
- HV filter directly on the PCB using a switchable common ground

# 2. Modelling the Charge Dispersion Phenomena

# Signal Formation

Anode Charge spreading

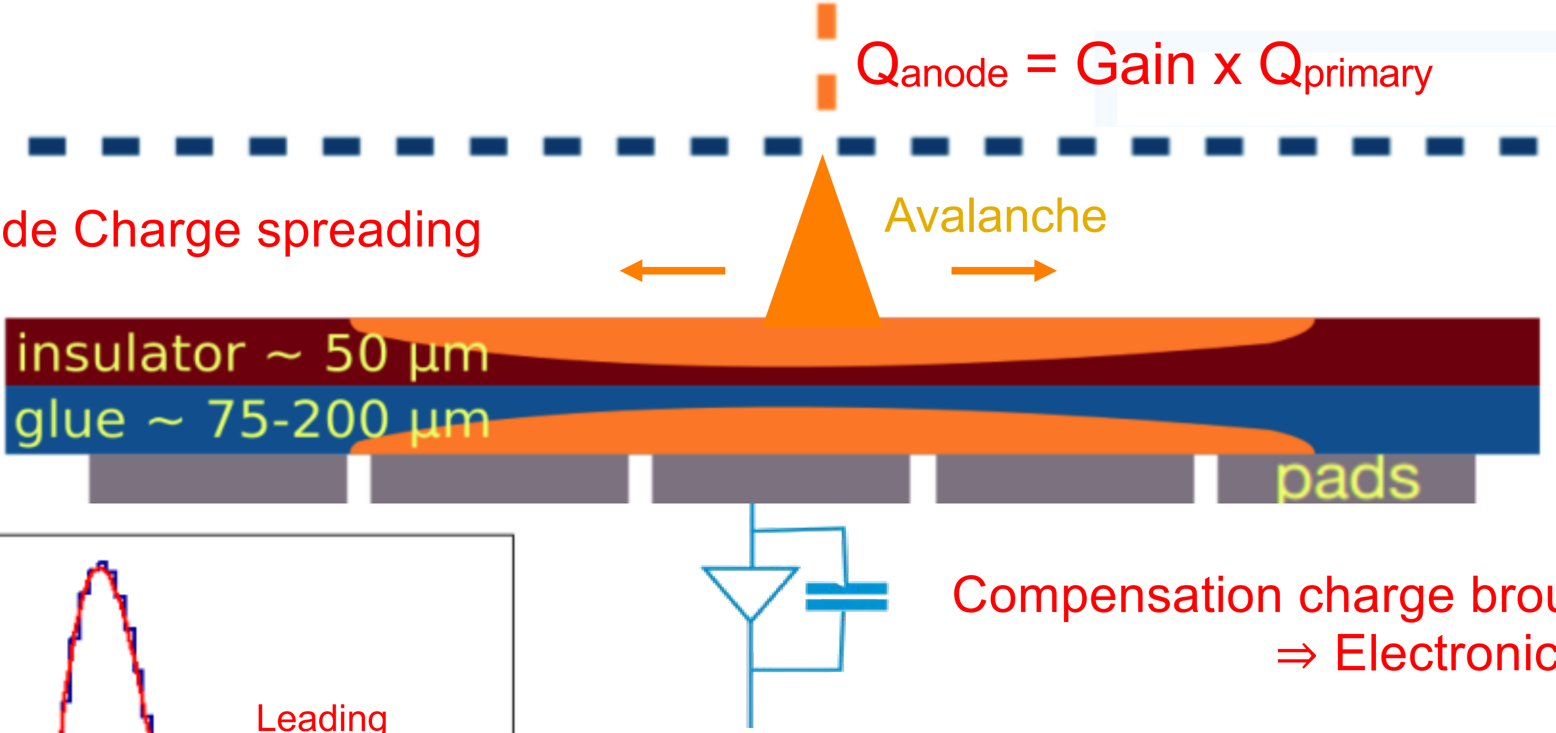


Capacitive DLC/pads coupling

Compensation charge brought on pads from ground
⇒ Electronics response

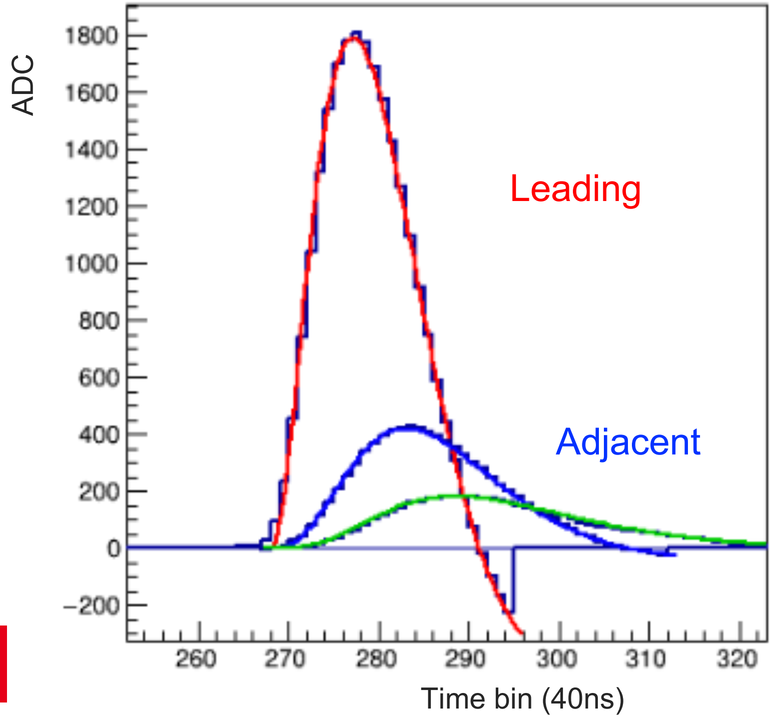


- **Leading pad**: highest and earliest signal → charge deposited in this pad
- **Adjacent pads**: lower and later signals → charge has diffused up and through these pads

# Charge Spreading

M.S. Dixit et.al., NIM A518, 721 (2004)
M.S. Dixit & A. Rankin, NIM A566, 281 (2006)

Resistance
+
capacitance
⇒ charge diffusion

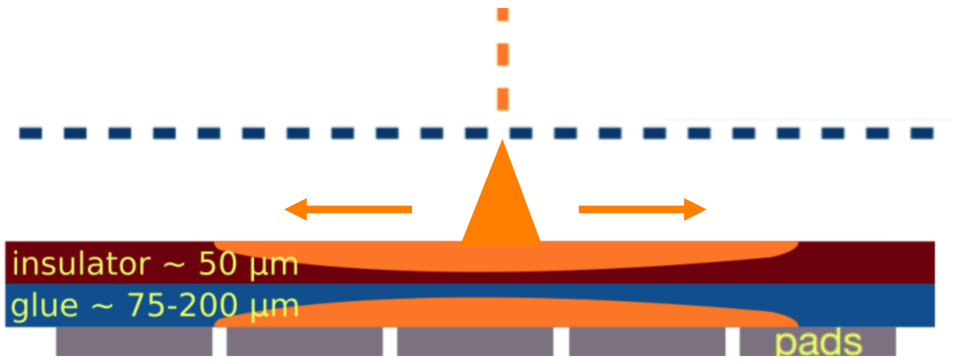


$$\frac{\partial\rho}{\partial t} = \mathrm{div}\vec{j_S},\ \vec{j_S} = \sigma\vec{E}, \vec{E} = -\nabla V \text{ and } V = \rho/C_S$$

$\sigma$ surface conductivity , $C_S$ surface capacitance

$$\Rightarrow \frac{\partial\rho}{\partial t} = \frac{1}{RC}\left(\frac{\partial^2\rho}{\partial^2 x} + \frac{\partial^2\rho}{\partial^2 y}\right) \text{ with } RC = \frac{C_S}{\sigma} \text{ in } s/m^2$$

**2D Telegrapher Equation**

Analytical solution for punctual charge deposition (assuming infinite DLC layer and uniform RC)

$$\rho_{punctal}(r,t) = \frac{Q_{anode}}{2\pi\sigma^2(t)} e^{\frac{-r^2}{2\sigma^2(t)}} \text{ where } \sigma(t) = \sqrt{\frac{2t}{RC} + w^2} \text{ and } w \text{ initial width (lateral diffusion)}$$

# Capacitive Coupling and Electronics Signal

Capacitive coupling means
a pad "responds" to the total charge on the resistive layer, lying directly above it

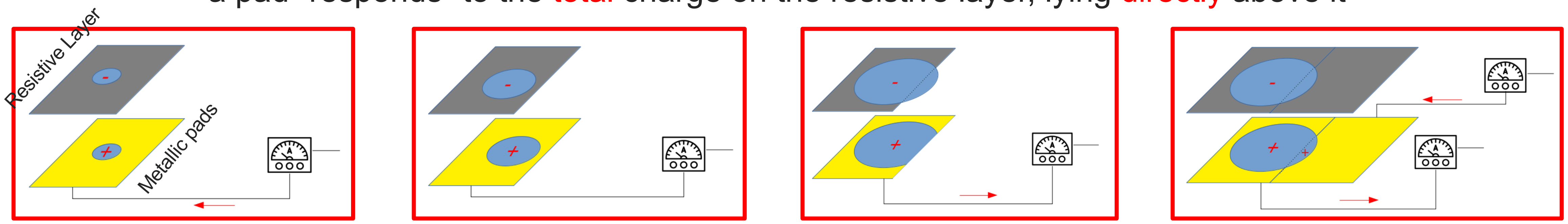


Electronic response : $ADC_{pad}(t) = \frac{dQ_{pad}}{dt} \otimes ADC^{Dirac} \quad (\Rightarrow ADC \neq Q)$

where $ADC^{Dirac}(t)$ is the electronic response to a Dirac pulse of current

# Capacitive Coupling and Electronics Signal

Capacitive coupling means
a pad “responds” to the total charge on the resistive layer, lying directly above it

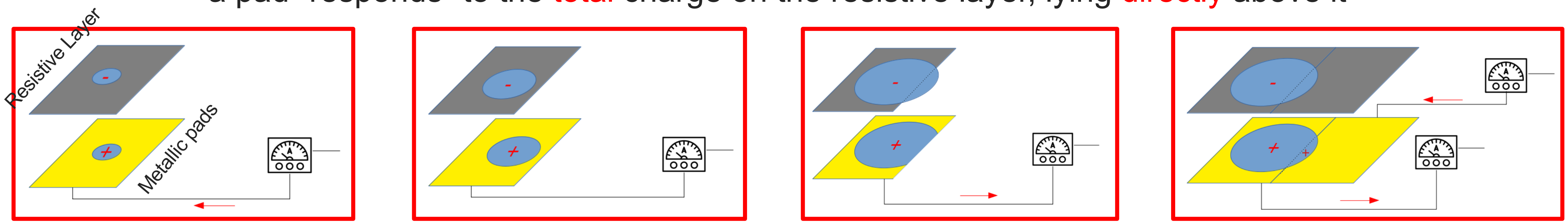


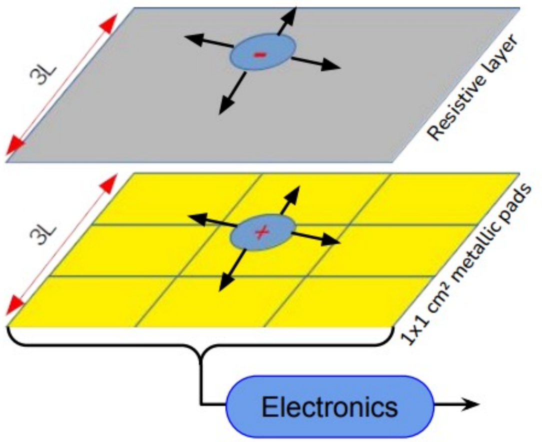


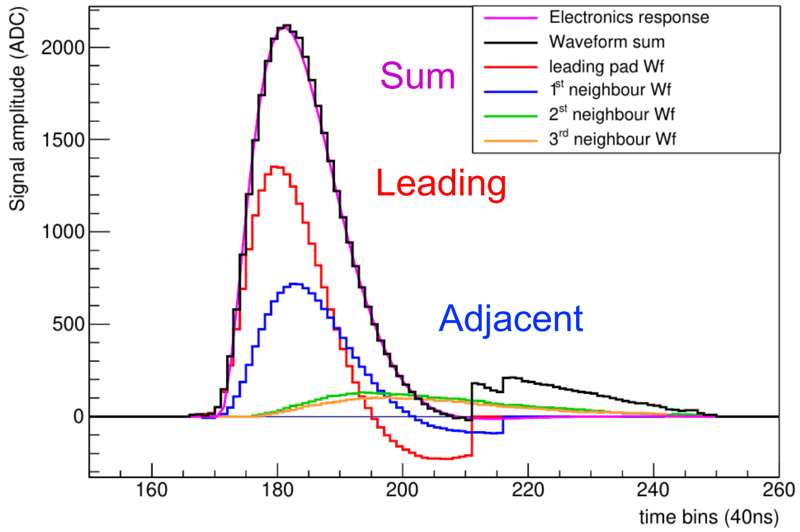

# Electronics Pulse Response

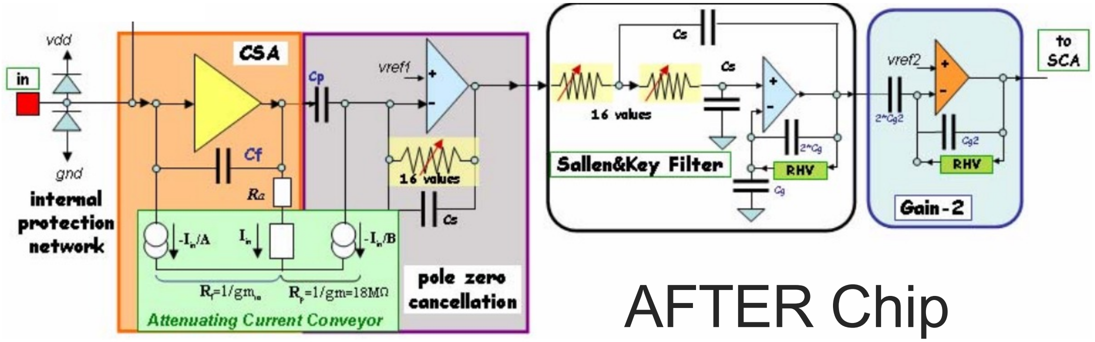


AFTER Chip

CA PZC Salen&Key Filter

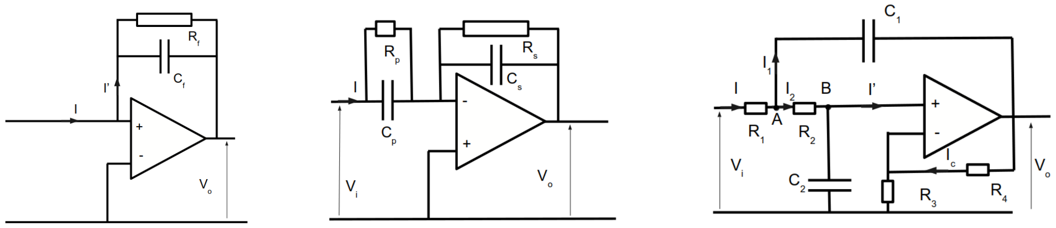

Laplace transform ⇒ pulse response

$$ADC^{Dirac}(t) = \frac{4096}{120fC}\frac{f(t;w_S,Q)}{f_{max}} \quad \text{where} \quad f(t;w_S,Q) = e^{-w_S t} + e^{\frac{-w_S t}{2Q}}\left[\sqrt{\frac{2Q-1}{2Q+1}}\,sin\left(\frac{w_S t}{2}\sqrt{4-\frac{1}{Q^2}}\right) - cos\left(\frac{w_S t}{2}\sqrt{4-\frac{1}{Q^2}}\right)\right]$$

Parametrization of the electronics response with 2 parameters

$w_S$~0.5/Peaking time and Q quality factor

# Validation of Electronic Model using Calibration data

- Each channel of an Electronics card is injected with multiple pulses of different amplitudes.
- Resulting output signals (response of Electronic cards) are fitted with the **Electronics response function.**
- Parameterized by two main variables related to shape of a signal waveform: **Q** and **$w_s$.**
- Variation in these fit parameters over all the pads was studied to determine if they can be set as constants.



$$R(t) = A\left[e^{-w_s t} + e^{\frac{-w_s t}{2Q}}\left(\sqrt{\frac{2Q-1}{2Q+1}}\sin\left(\frac{w_s t}{2}\sqrt{4-\frac{1}{Q^2}}\right) - \cos\left(\frac{w_s t}{2}\sqrt{4-\frac{1}{Q^2}}\right)\right)\right]$$

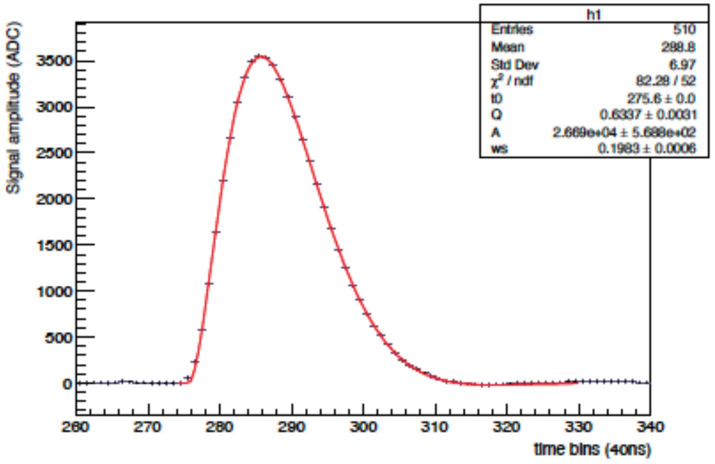


## Q map

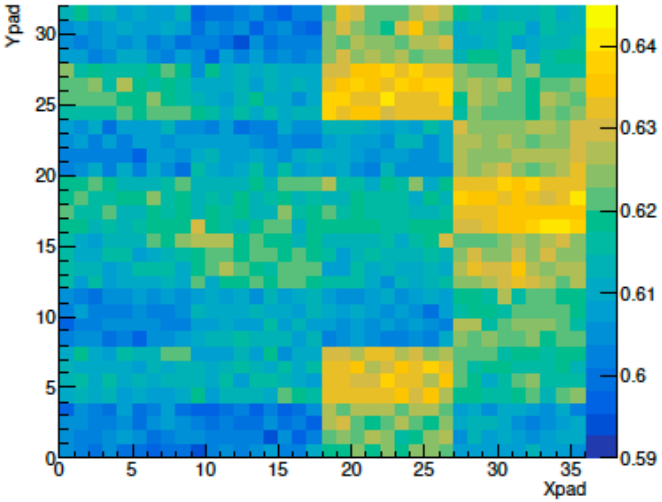


## $w_s$ map

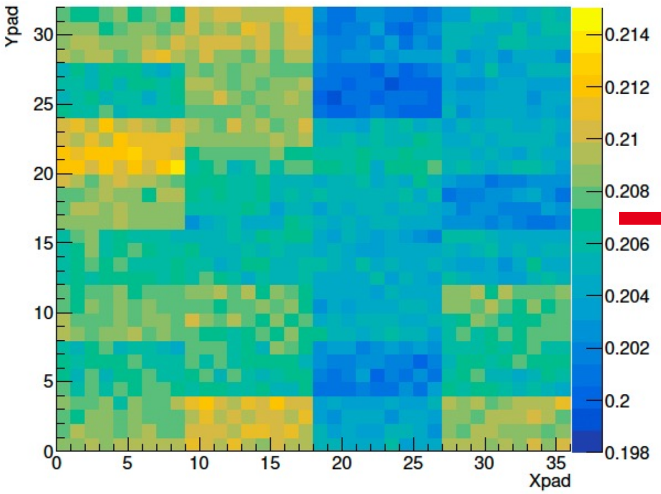


Fixed

$Q = 0.6368$

$w_s = 0.1951$

# 3. RC and Gain Measurements using X-rays Data

# ERAM Tests with X-rays at CERN

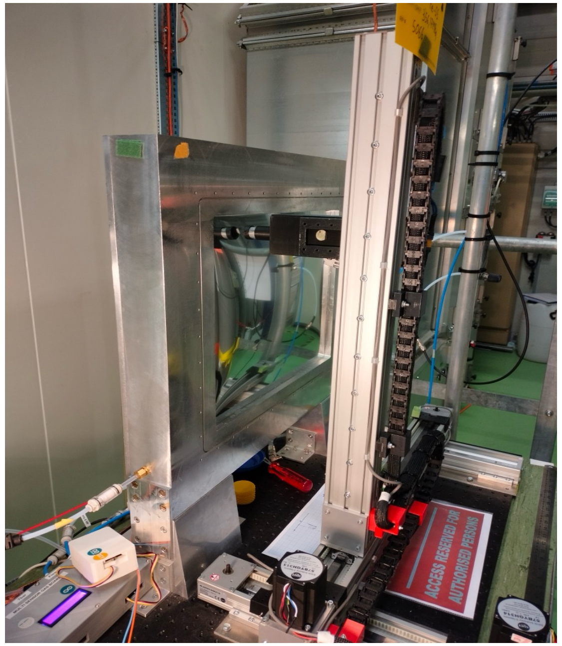

- Each pad(1152) of an ERAM placed inside an X-ray chamber (3 cm drift) is scanned using a robot holding an $^{55}Fe$ X-ray source.
- Charge is deposited in targeted pad and its neighboring pads (due to charge spreading), from electron avalanche caused by an X-ray photon.
- $^{55}Fe$ spectrum can be reconstructed using all events in one pad → Summing all waveforms in each event and taking amplitude max of summed waveforms
- **Gain value** is obtained for a pad by fitting its $^{55}Fe$ spectrum. Resolution of 10% is obtained.

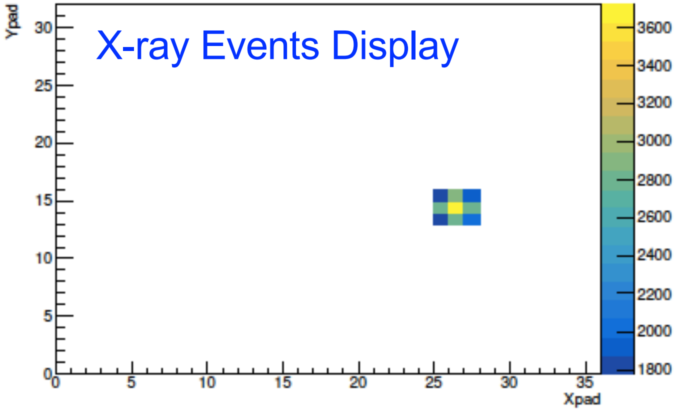


Example of a $^{55}Fe$ spectrum in 1 Pad

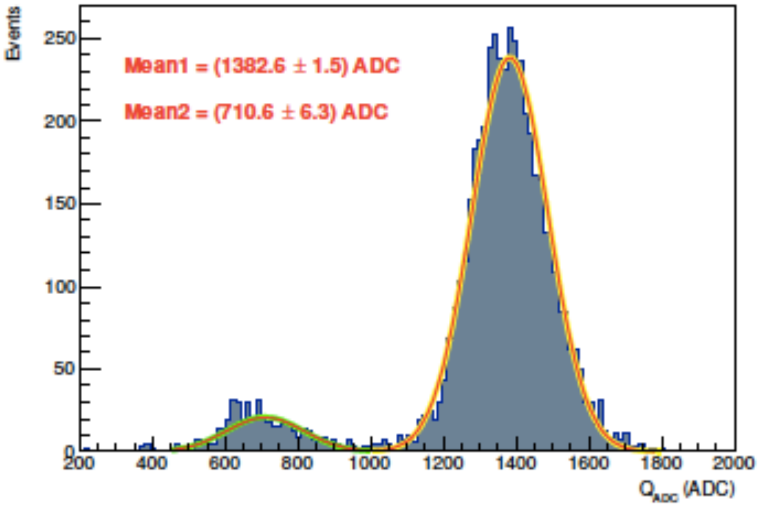

# Charge Spreading Template

Qpad(t) = Integration of 2D Teq. for diffusion of initital Qe deposited charge (point-like, delta-pulse initial conditions)

- Integrating charge density function over area of one readout pad.

$$Q_{pad}(t) = \frac{Q_e}{4} \times \left[ erf\left(\frac{x_{\text{high}} - x_0}{\sqrt{2}\sigma(t)}\right) - erf\left(\frac{x_{\text{low}} - x_0}{\sqrt{2}\sigma(t)}\right) \right] \times \left[ erf\left(\frac{y_{\text{high}} - y_0}{\sqrt{2}\sigma(t)}\right) - erf\left(\frac{y_{\text{low}} - y_0}{\sqrt{2}\sigma(t)}\right) \right]$$

$$\sigma(t) = \sqrt{\frac{2t}{RC} + \omega^2}$$

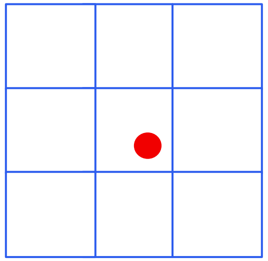

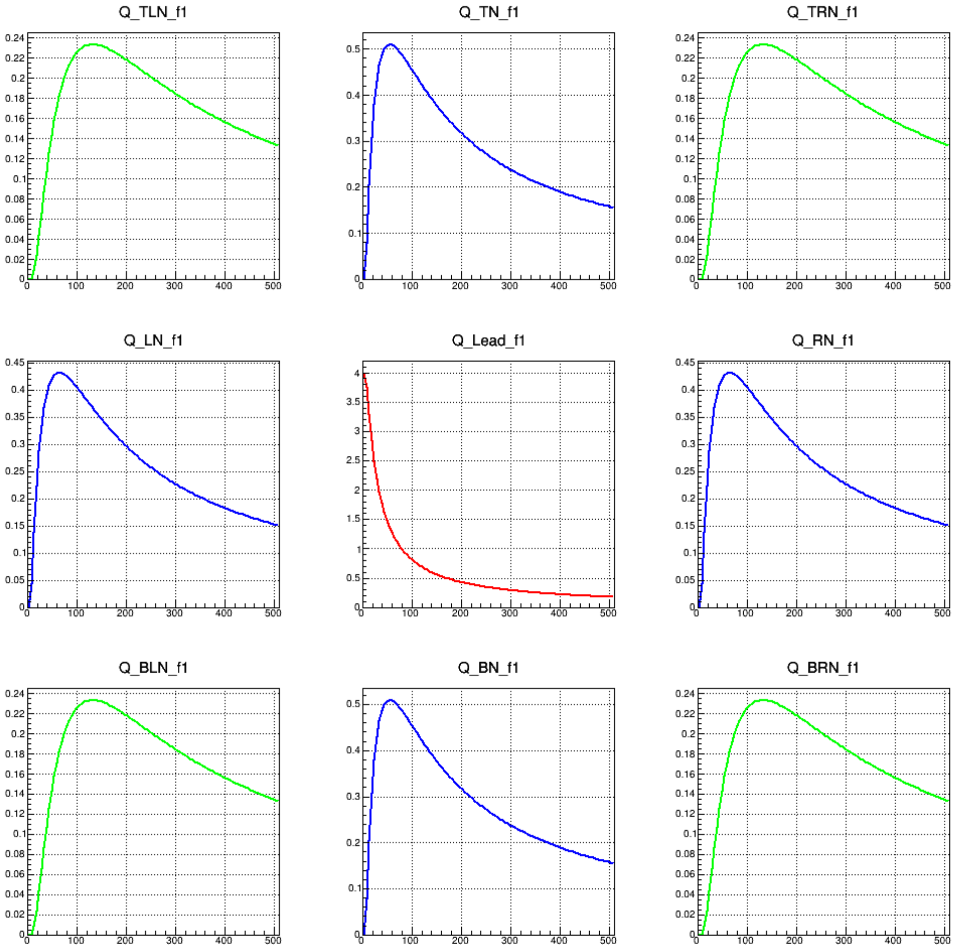


- **Parameterized by 5 variables:**
  - $x_0$ } Initial charge position
  - $y_0$
  - $t_0$ : Time of charge deposition in leading pad
  - RC : Describes charge spreading
  - $Q_e$ : the initial charge after charge multiplication in the amplification

# Signal Model Template

Convolution of charge diffusion function with derivative of electronics response function.

$$S(t) = Q_{pad}(t) \circledast \frac{\mathrm{d}(ADC^D(t))}{\mathrm{d}t}$$

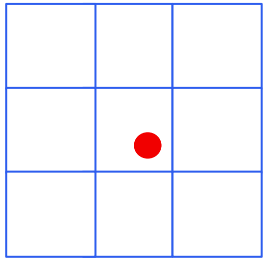

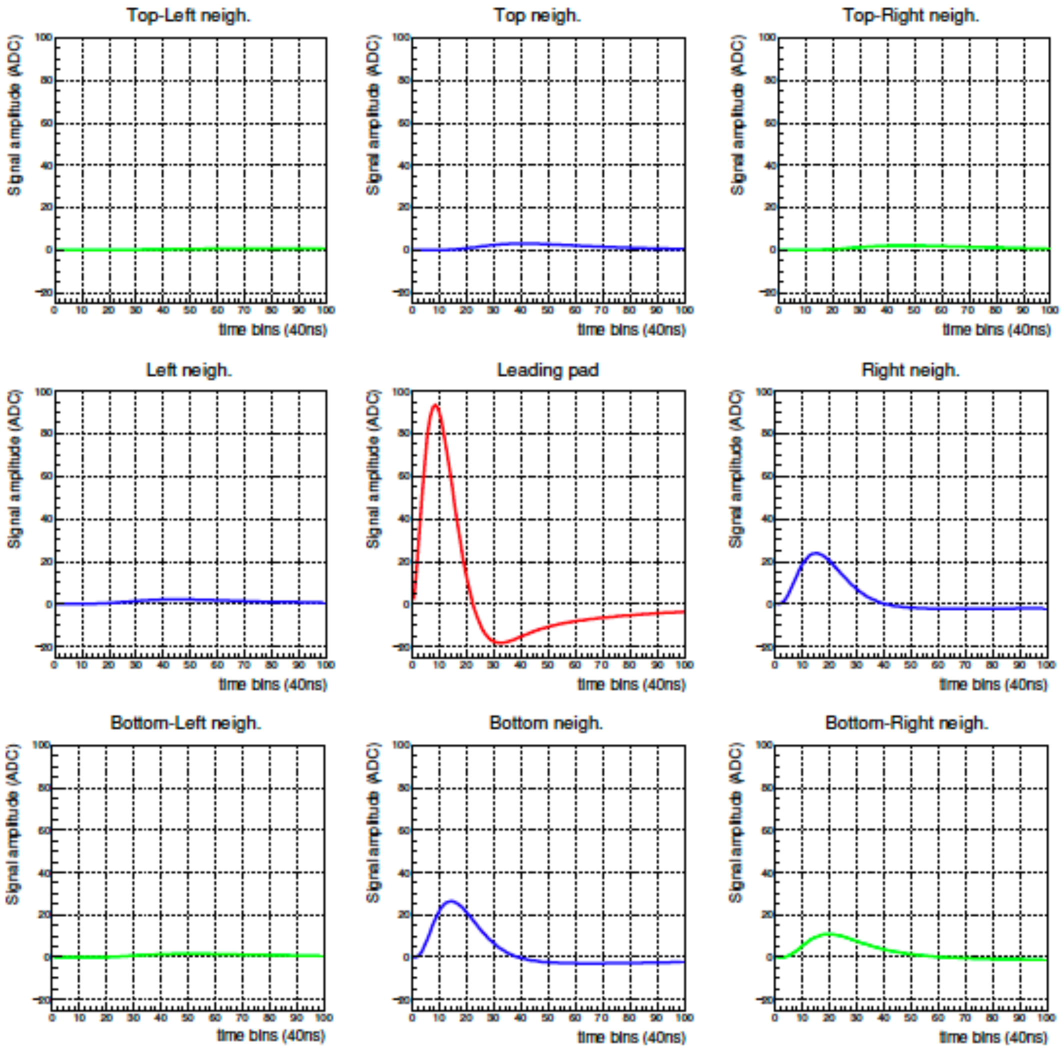

# Application of Signal model on X-ray data

Example 1 of Simultaneous Fit of Waveforms

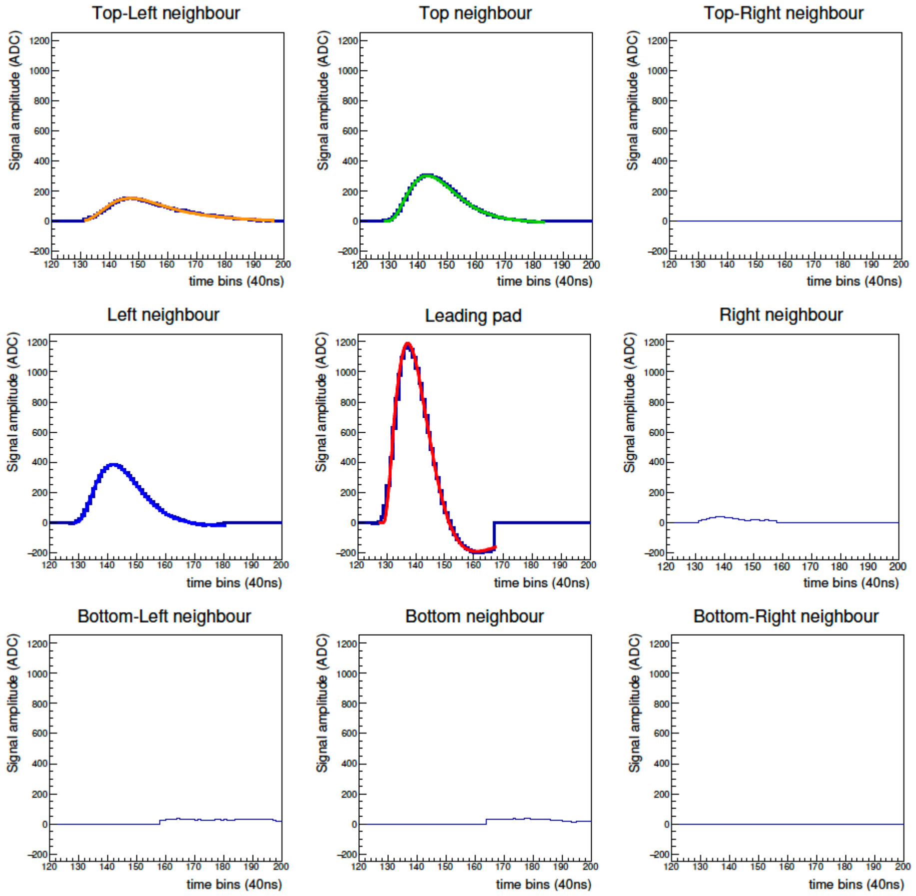


Example 2 of Simultaneous Fit of Waveforms

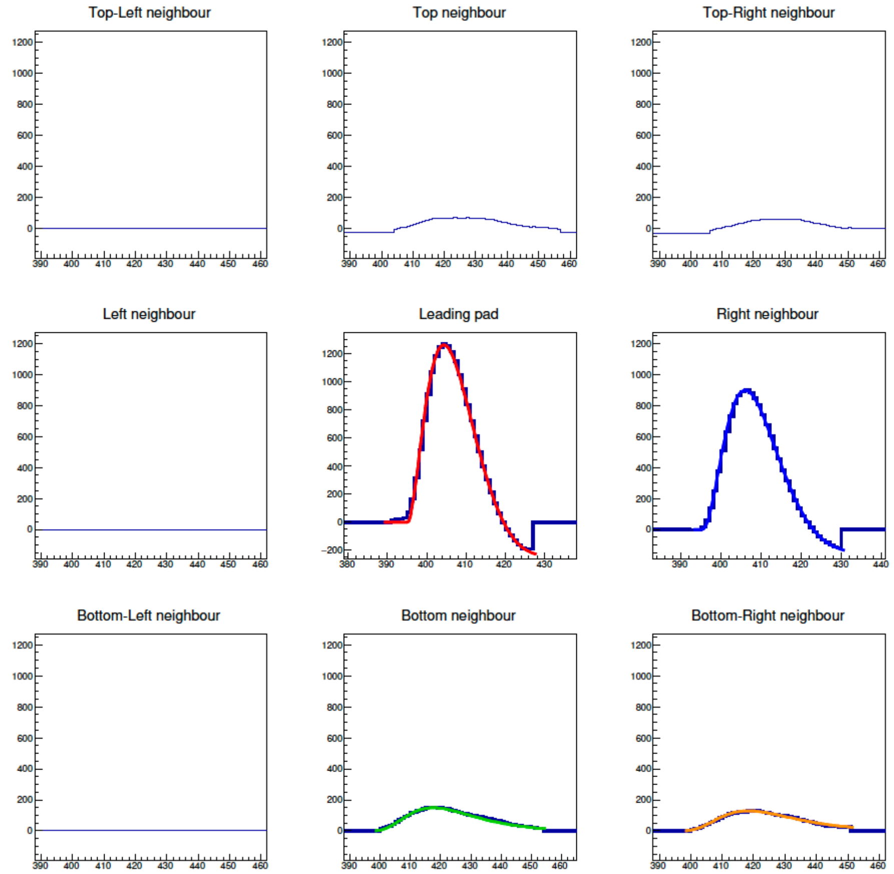


Fit results: $RC$ = $(146.6 \pm 1.6)$ ns/mm$^2$, $Q_e$ = $(327.6 \pm 1.8) \times 10^3 e$, $(x_0, y_0)$= (-0.442 cm, 0.352 cm) (w.r.t center of leading pad) , $\chi^2$/Ndf = 1.08.

Fit results: $RC$ = $(100.5 \pm 1.1)$ ns/mm$^2$, $Q_e$ = $(405.9 \pm 2.1) \times 10^3 e$, $(x_0, y_0)$ = (0.523 cm, -0.108 cm)(w.r.t center of leading pad), $\chi^2$/Ndf = 1.48

# Application of Signal model on X-ray data

Example 1 of Simultaneous Fit of Waveforms

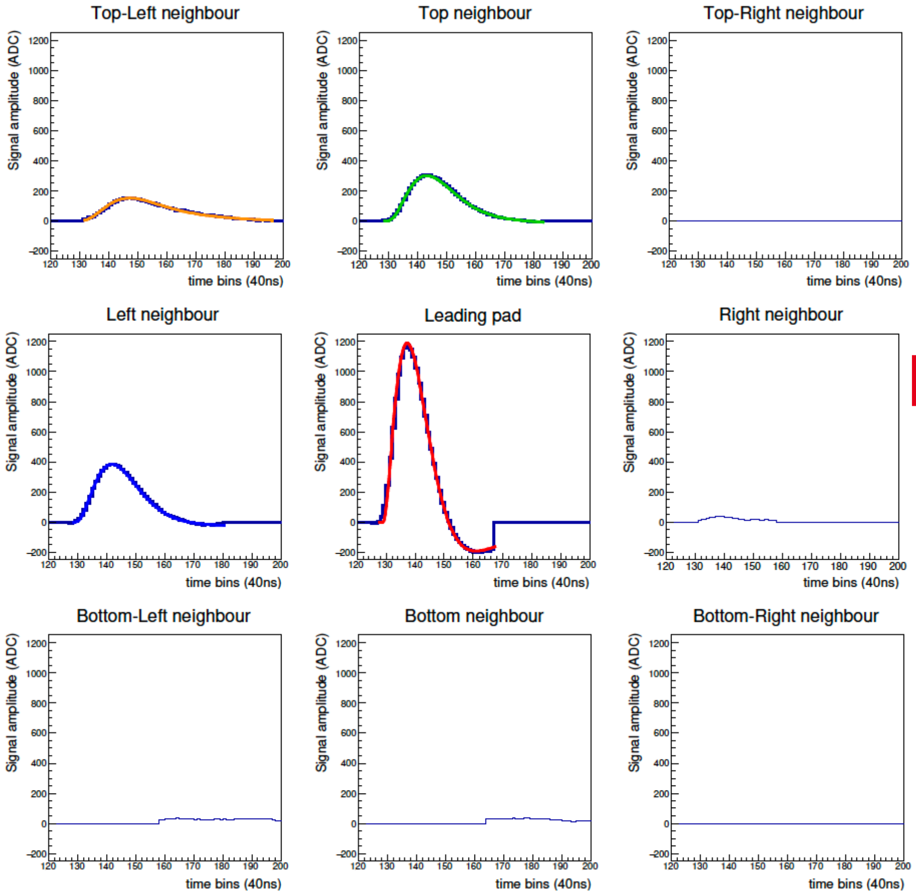


RC distribution

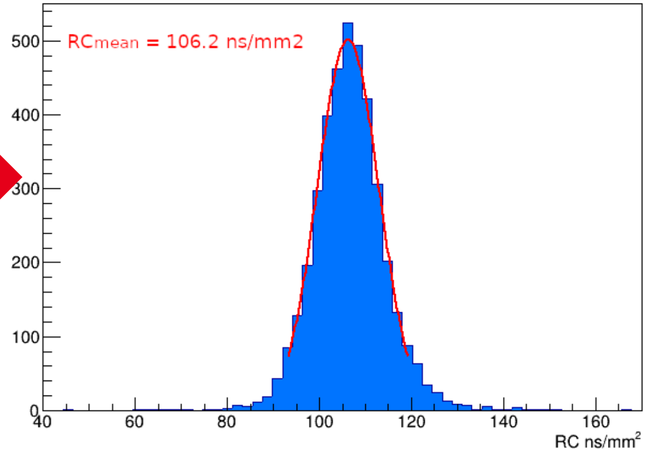


$Q_e$ distribution

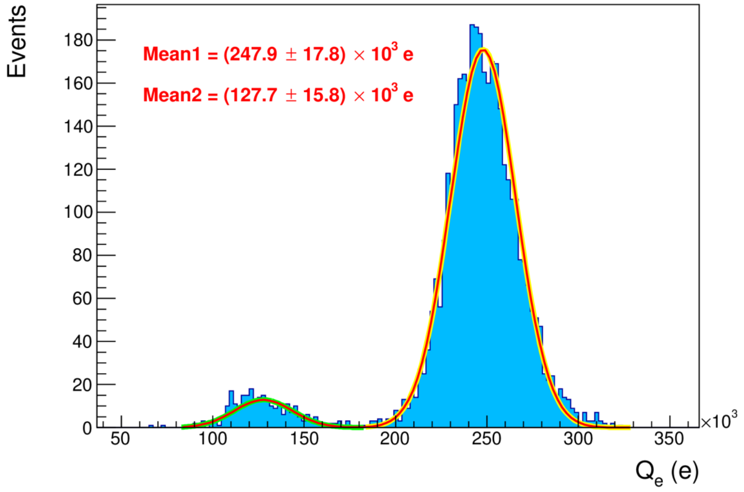


$Q_e$ distribution reproduces $^{55}Fe$ spectrum→Extract Gain

Fit results: $RC$ = $(146.6 \pm 1.6)$ ns/mm$^2$, $Q_e$ = $(327.6 \pm 1.8) \times 10^3 e$, $(x_0, y_0)$= (-0.442 cm, 0.352 cm) (w.r.t center of leading pad) , $\chi^2$/Ndf = 1.08.

# Validation of Signal Model

## Cross-check Gain with an other method

Gain map from waveform fit

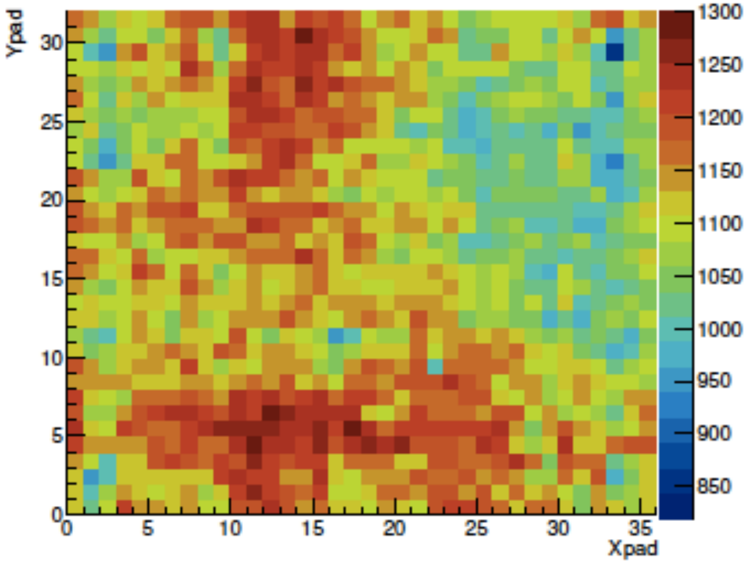


Gain map from sum of waveforms

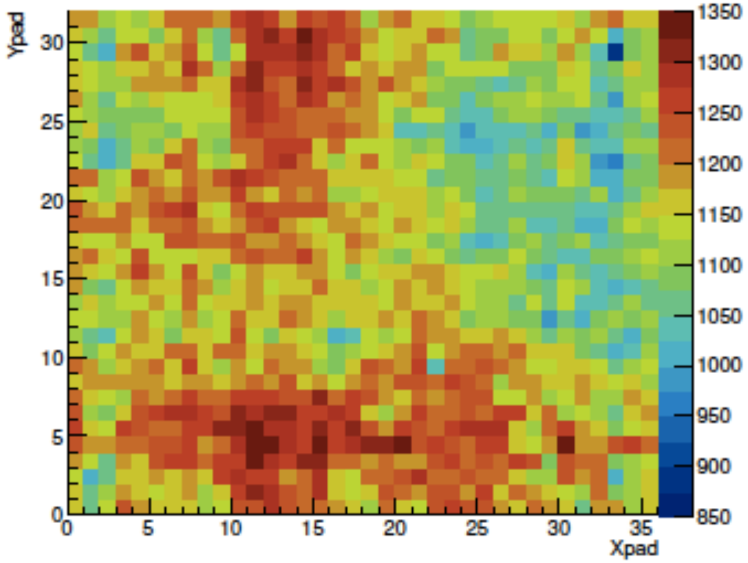


Ratio of Gain(of each pad) obtained from 2 different methods

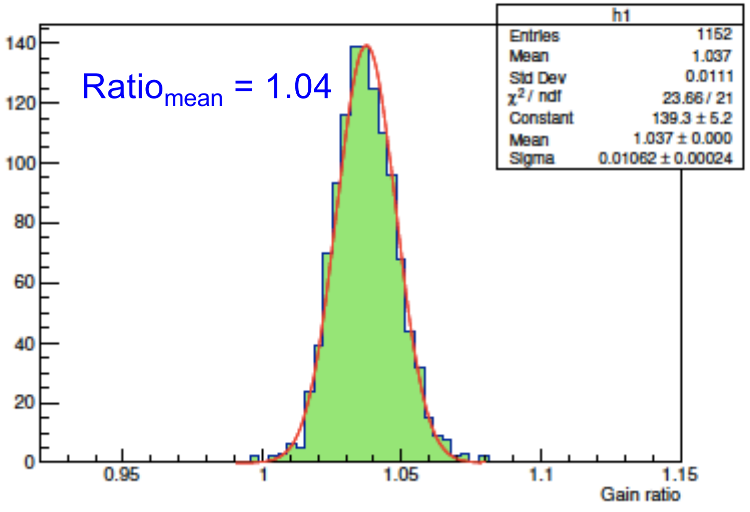


- Very high similarity in gain maps obtained from two different methods.
  - Method 1: fit of the waveforms using the analytical model
  - Method 2: fit of $^{55}Fe$ spectrum obtained by summing all waveforms in each event and taking amplitude max of summed waveforms.
- Gain results serve as validation for Electronics Response function, and robustness of entire model.

# RC maps for different ERAMs in one readout plane

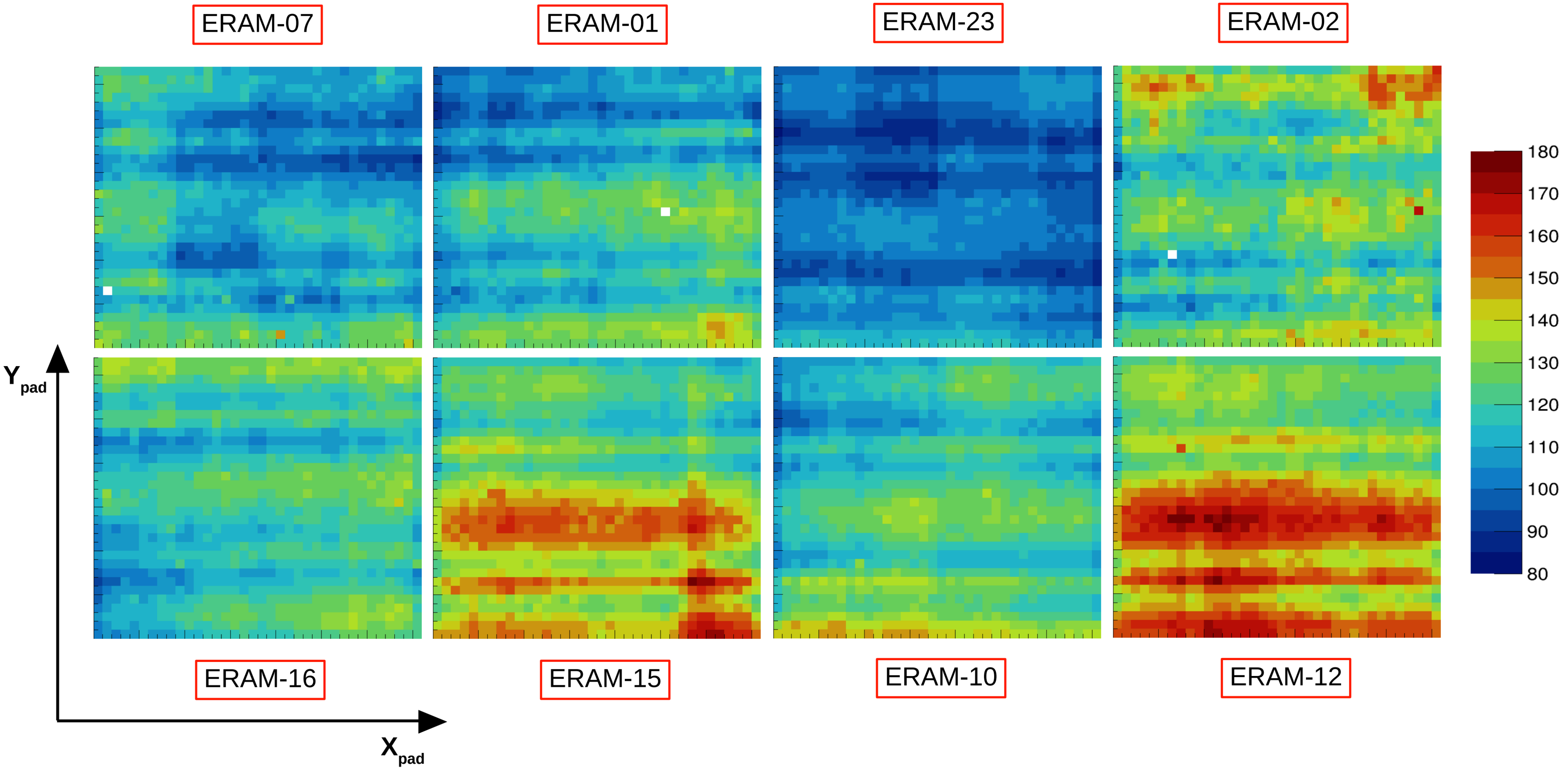

# Understanding RC map : Comparaison with Resistivity (R) measurements

ERAM-PCB: Resistivity measurements

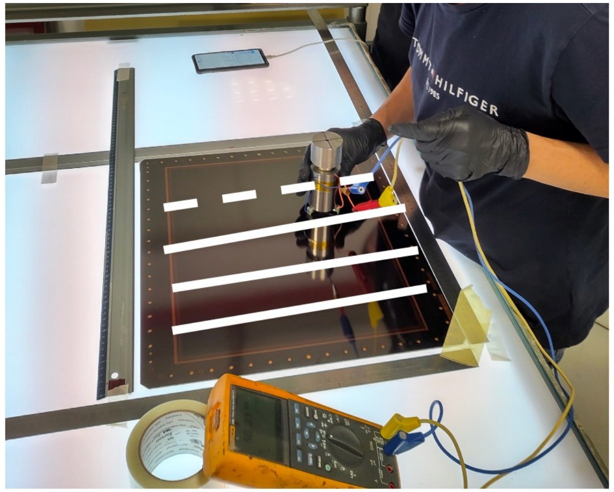

ERAM-PCB: Resistivity measurements

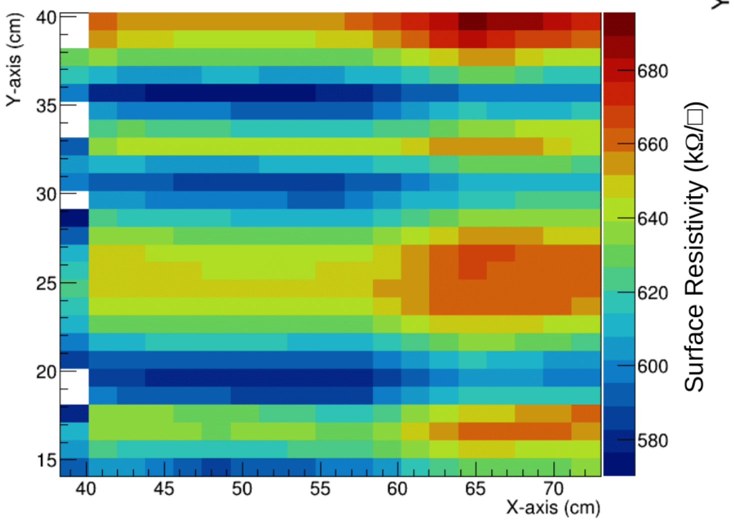


ERAM-16: RC map from fit

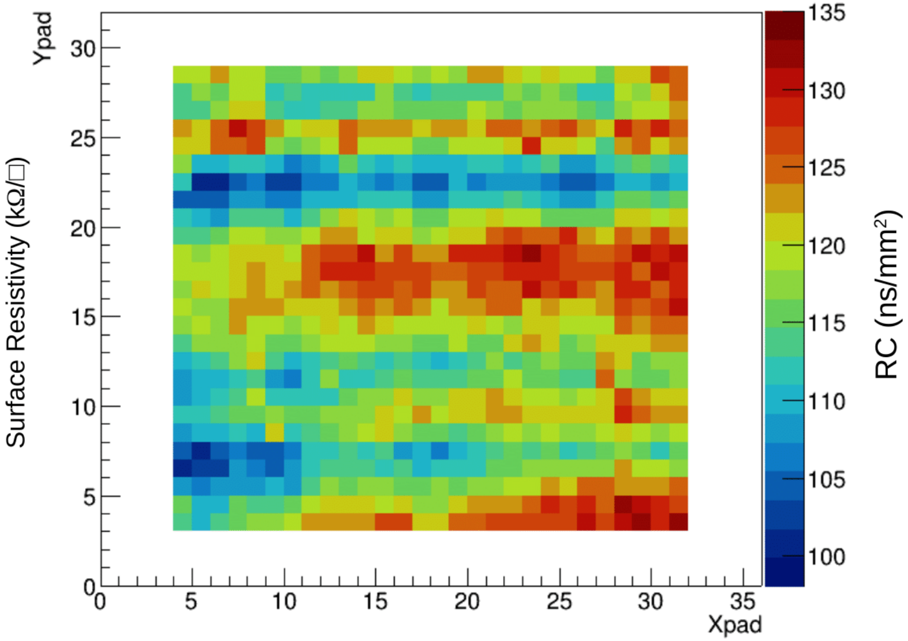


- Performed 90 R-measurements → 18 rows x 5 columns using dedicated probe.
- RC map structures seem to be correlated with R measurements (C is very well constrained by the thickness of insulator).
- R inhomogenities in the sputtering are clearly visible in the direction perpendicular to the drum rotation axis.

# Gain maps

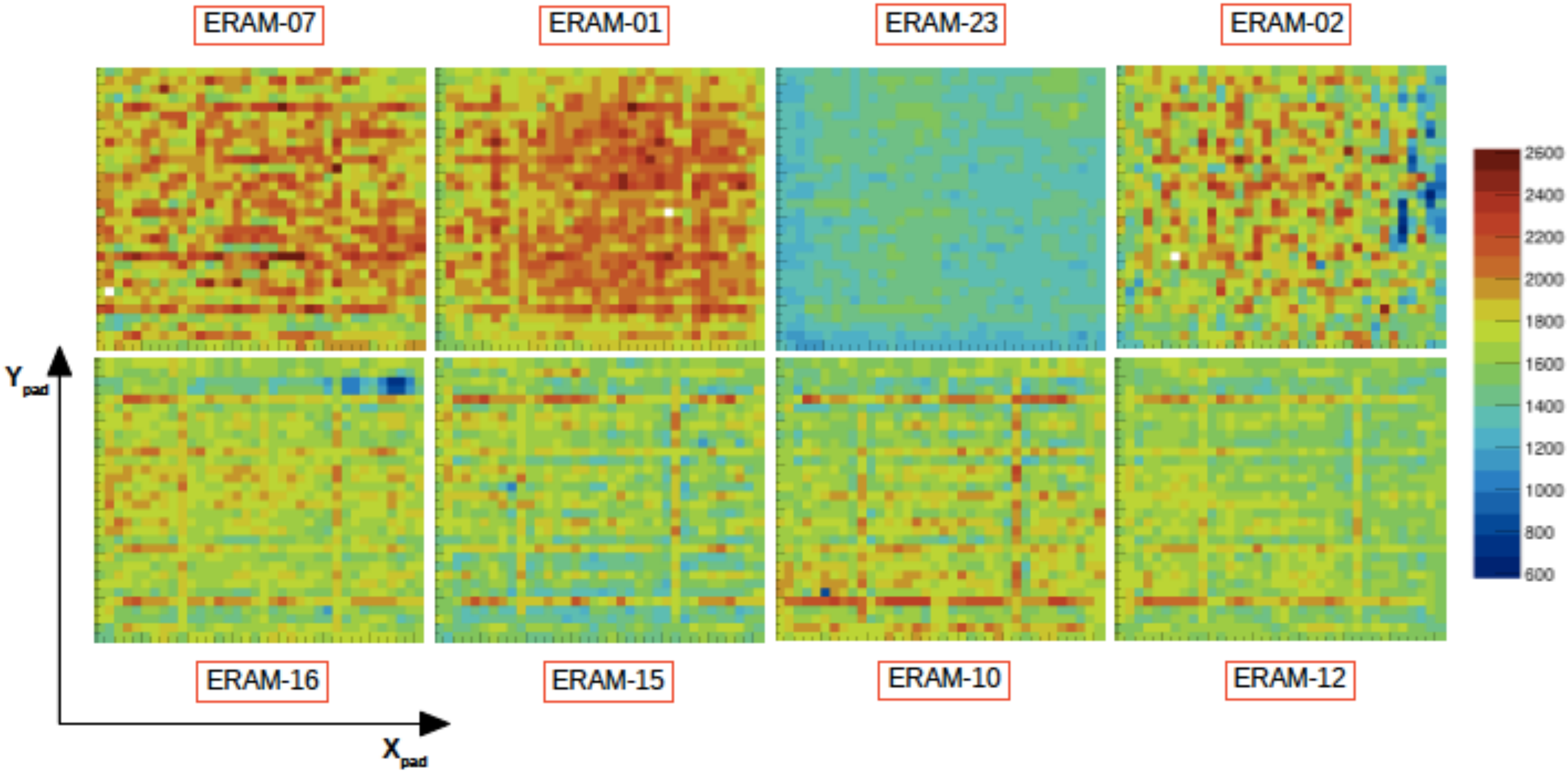


Various PCB designs were visible due to mechanical ribs, but this issue has been resolved since ERAM-23.

# Understanding Gain maps

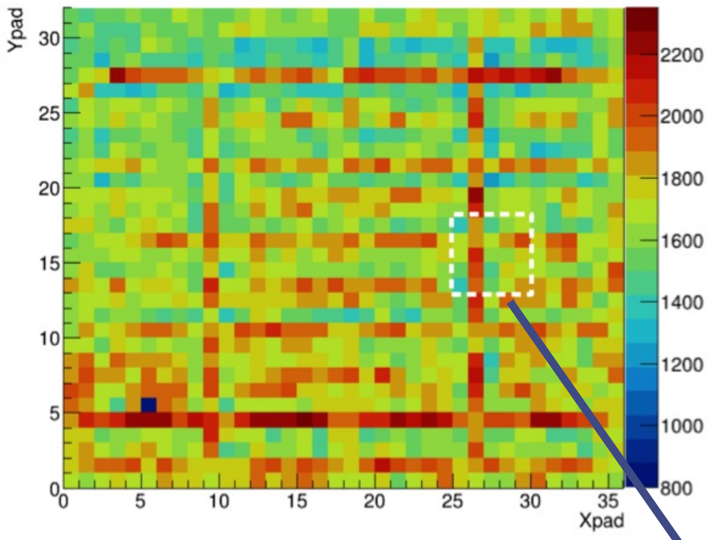


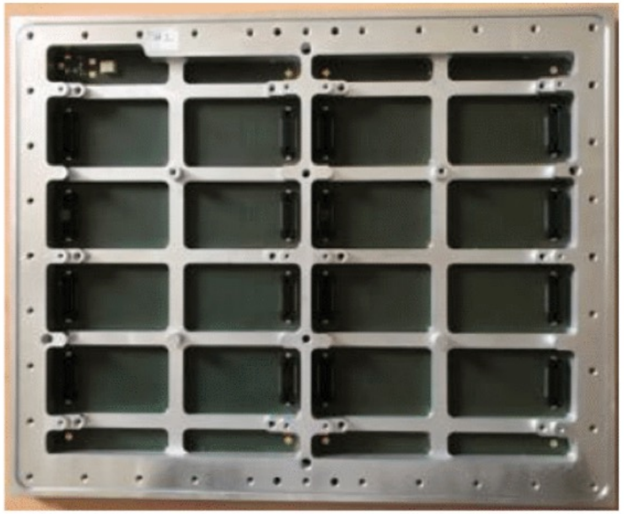

- Change of PCB design provided the solution
- Removal of an insulating layer on the PCB
- 1 $\mu$m mesh-DLC gap variation → 10% variation in gain

Visualization of gain non-uniformity within pads located over PCB stiffener, with high granularity, made possible due to the excellent position resolution obtained with the simultaneous fit method

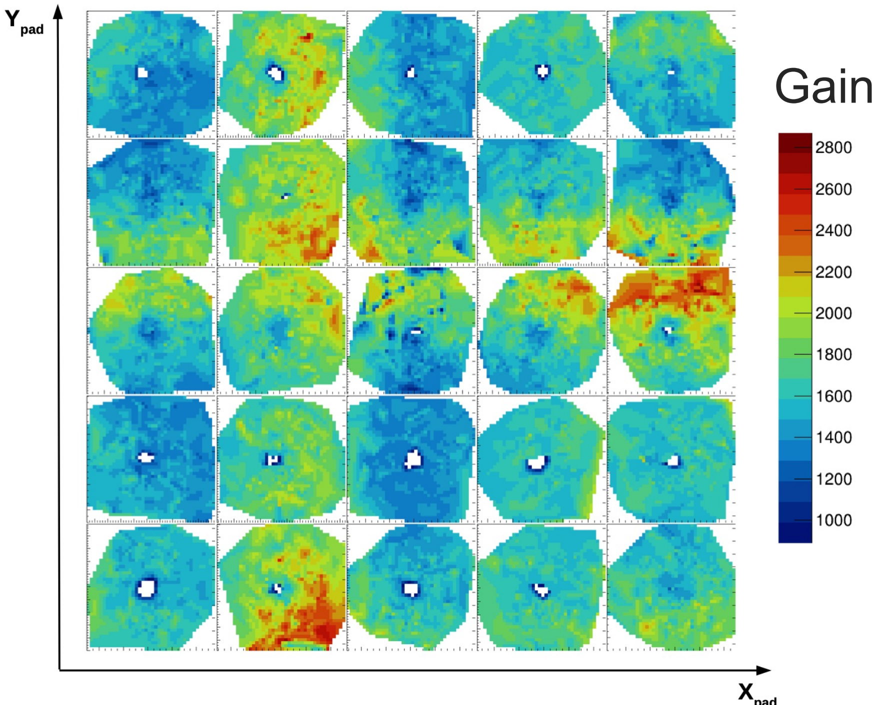

# Production and Charaterization of 37 ERAMs

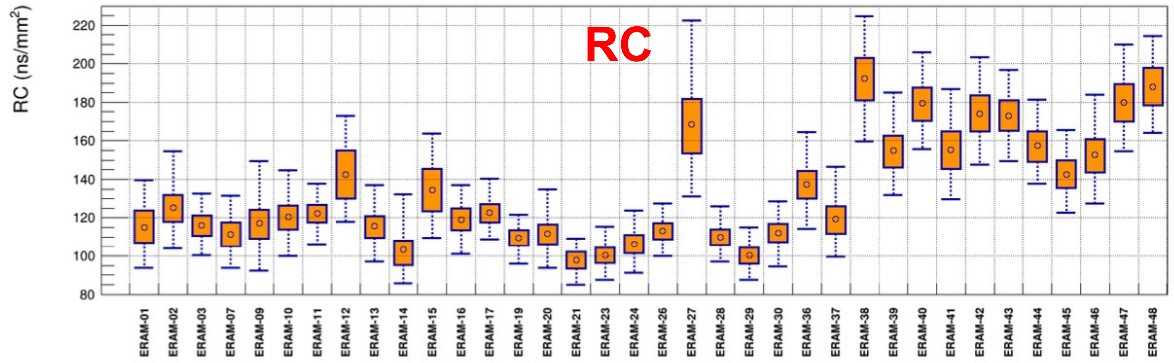


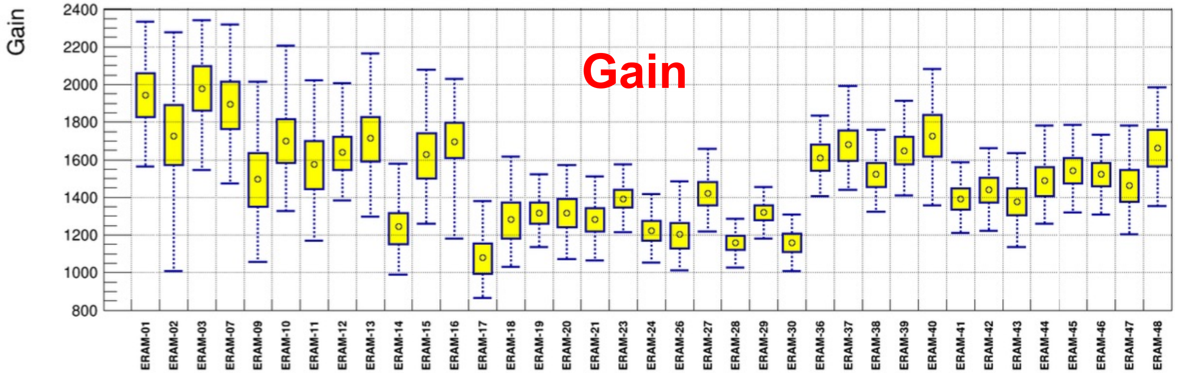


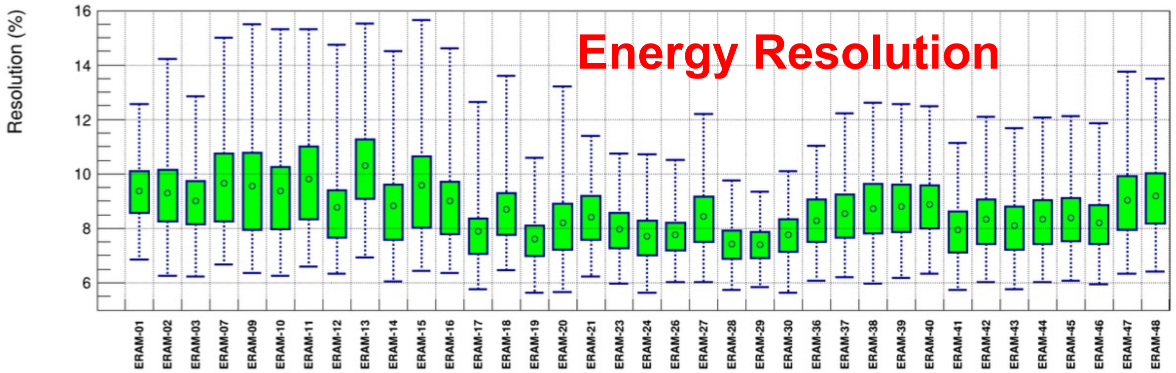


No correlation between mean RC and Gain of analyzed ERAMs.

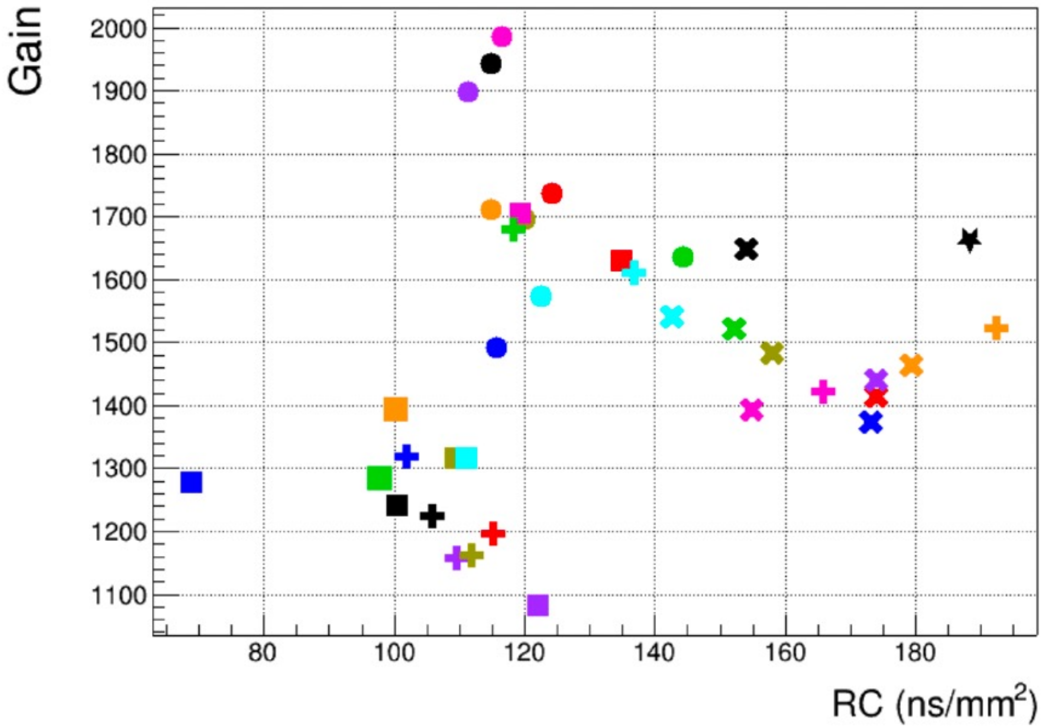


Lower and upper bounds of box: [Mean – 25%, Mean + 25%] of distribution (50% of values within box).
Lower and upper bounds of bars: [Mean – 49%, Mean + 49%] of distribution (98% of values within bars).

# 4. Understanding the Noise

# Understanding the Noise

To understand the signal, one has to understand the noise. So how it looks?

Record of the baseline (no trigger)

One record
$T_p$= 412 ns
$F_s$ = 25 MHz

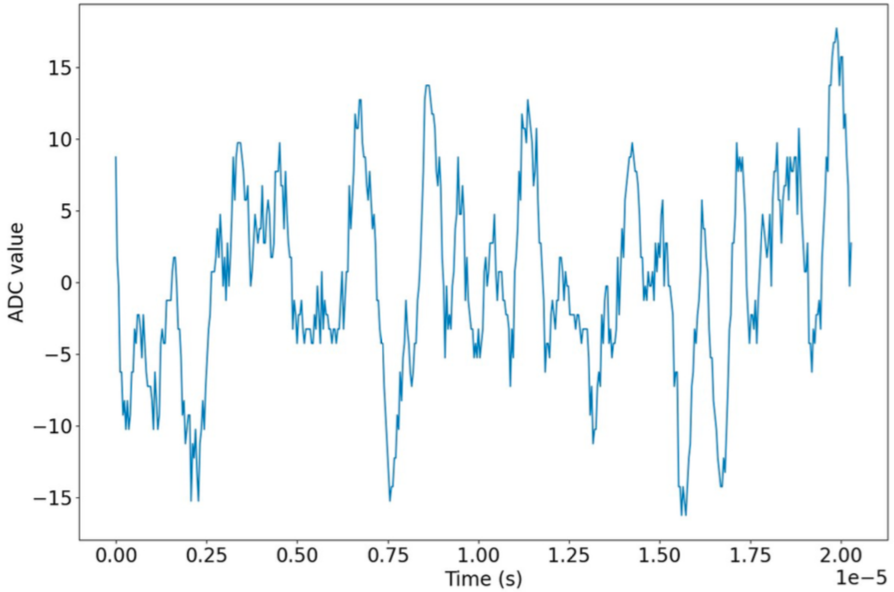


Fluctuations over many time bins

⇒ The frequencies of the bulk of Noise are much lower than 25 MHz (1/time bin)

⇒ Low frequency noise

Done 10 times for all pads of the 16 Erams now in situ (bottom TPC), for 4 sampling frequencies and 2 peaking times

# Understanding the Noise

Mean FFTs over the 10 events for each pad for the 16 ERAMs

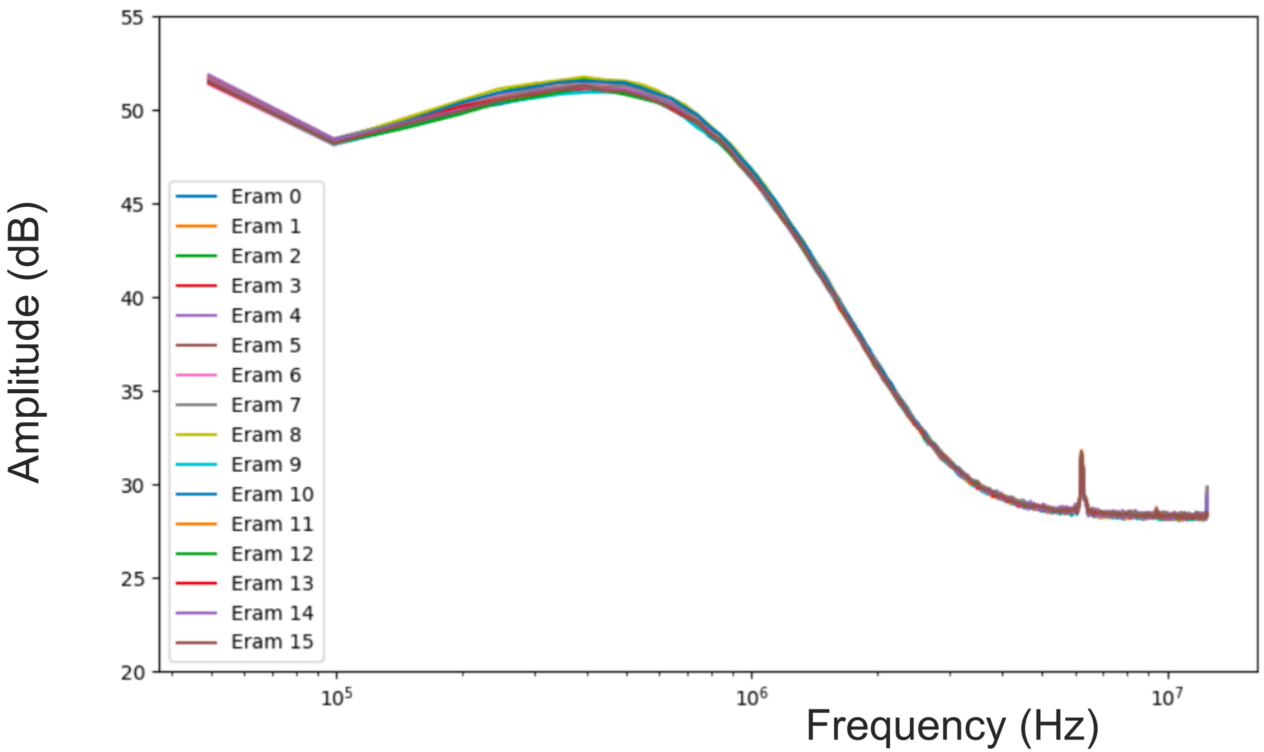


Comparaison of averages over all erams of a module

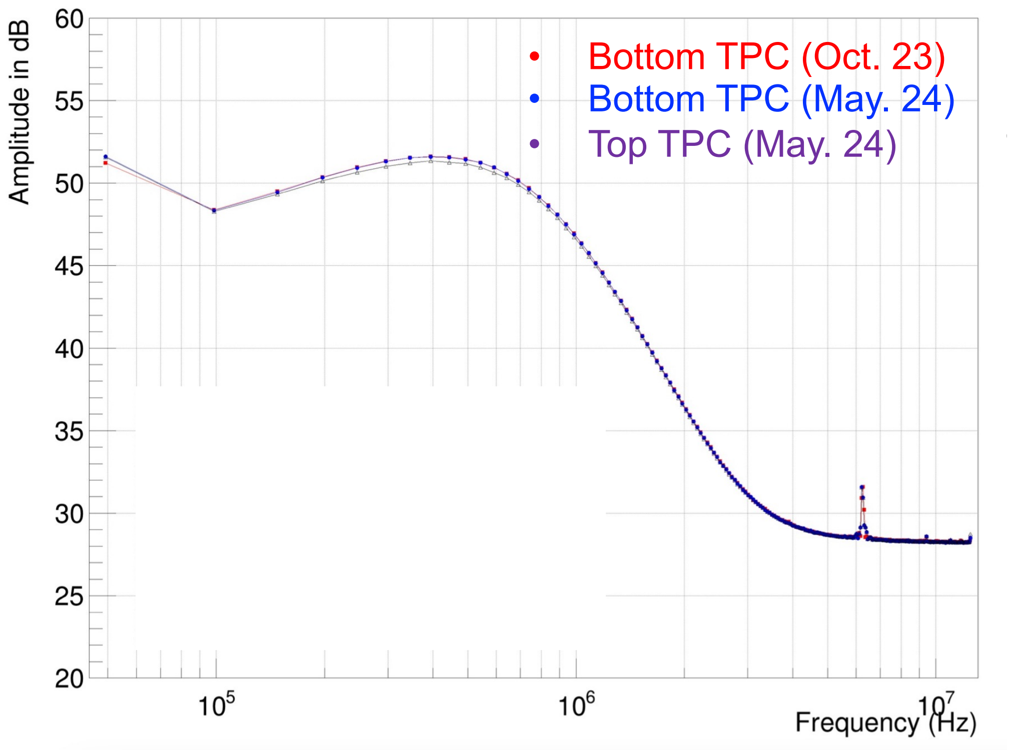


- All the Erams have quasi-identical noise level which is stable in time.
- The nearly identical noise levels across all ERAMs reflect :
  - the excellent uniformity of the electronics and the mechanical definition of the glue layer driving the detector capacitance.

# Three Noise Components

Averaged waveform over all Erams and time bins

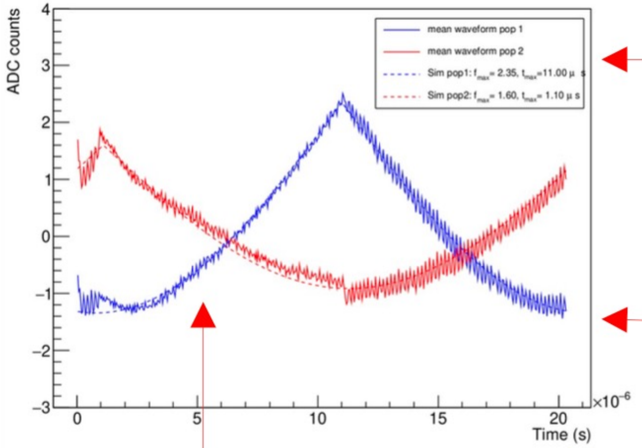


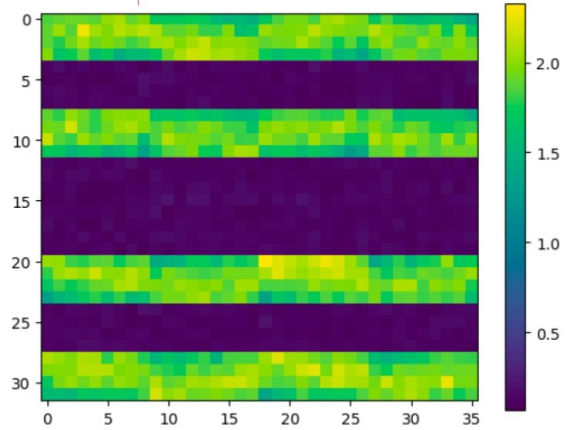

2 populations on each ASIC

Fast Fourrier Transform

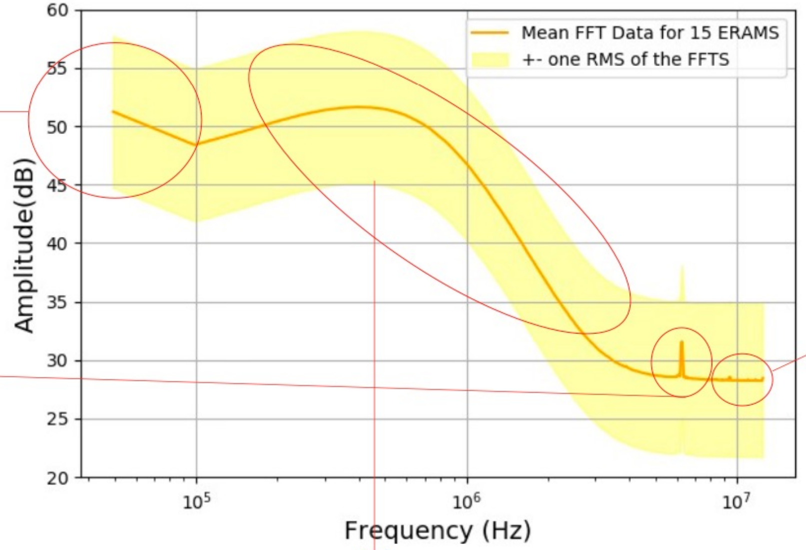


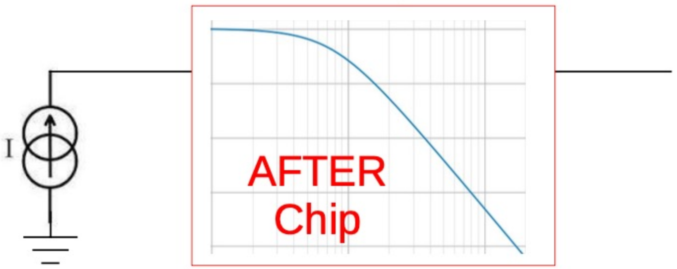


The Bulk of the spectrum

$$ADC(t) = I_{input} \otimes AFTER_{pulse}$$

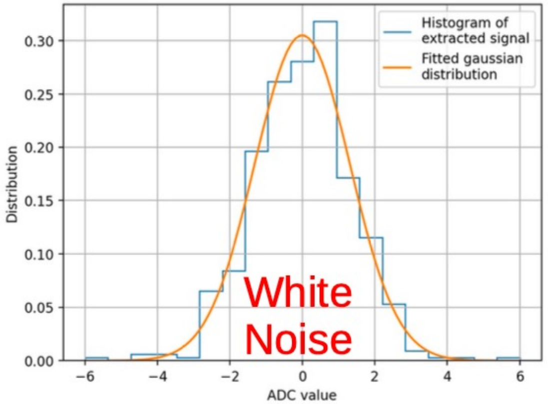


Constant Power Spectral Density
$\sigma$ ~1 ADC

Noise Model built

# Understanding the Noise: Making noise

Mean Fourier transforms of the real data compared to Toy model

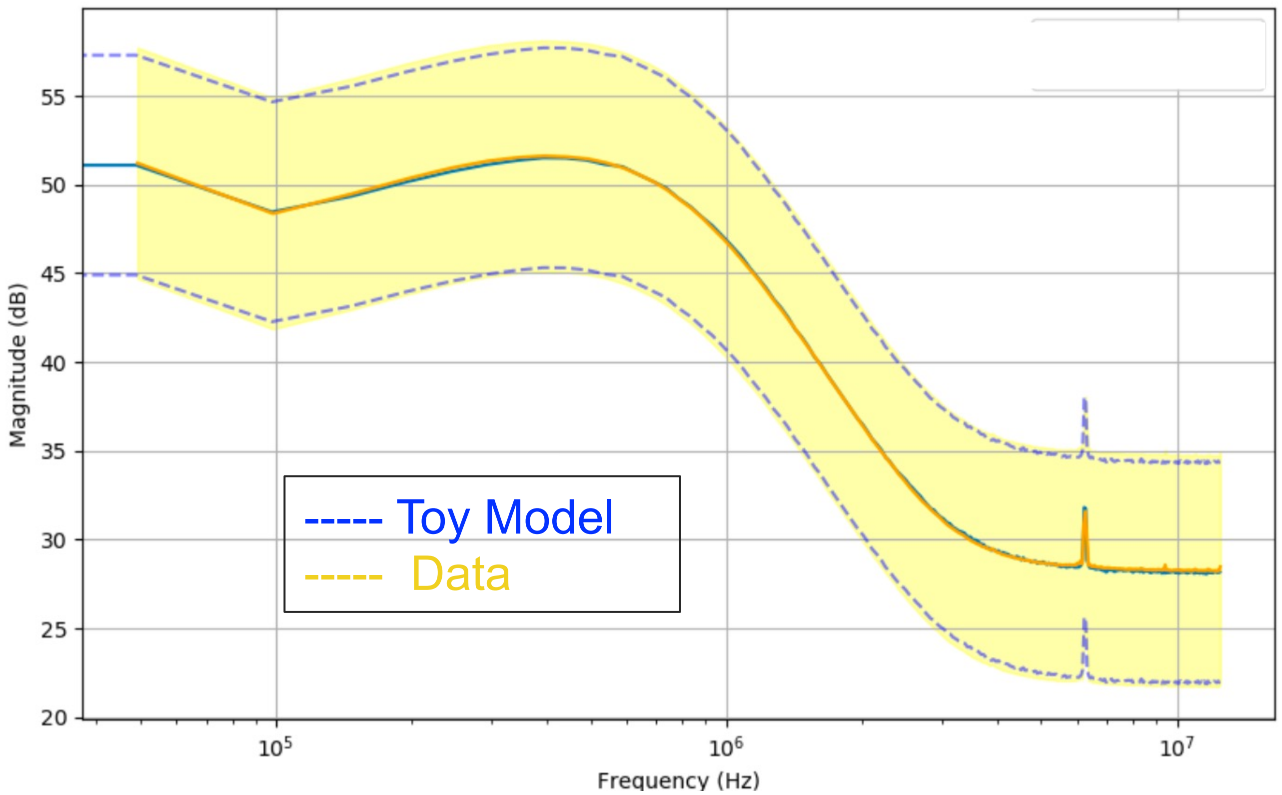


- Produce toys samples by generating 10-k waveforms (510 time bins) based on our noise model.
- The real data is almost perfectly reproduced.

# Understanding the Noise:  Making Noise

data

X-ray data waveforms

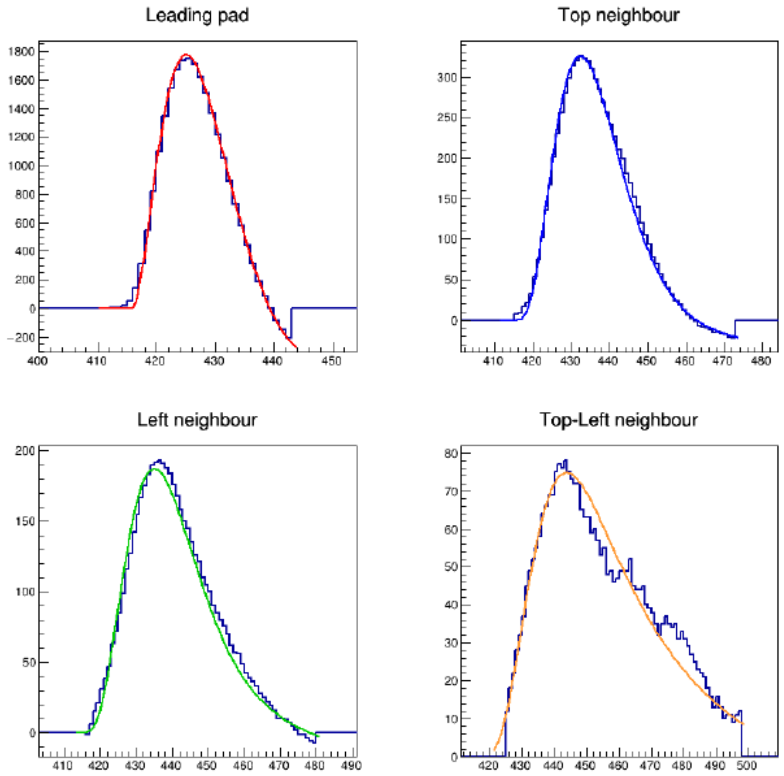


Very realist simulation

Simulated noisy waveforms

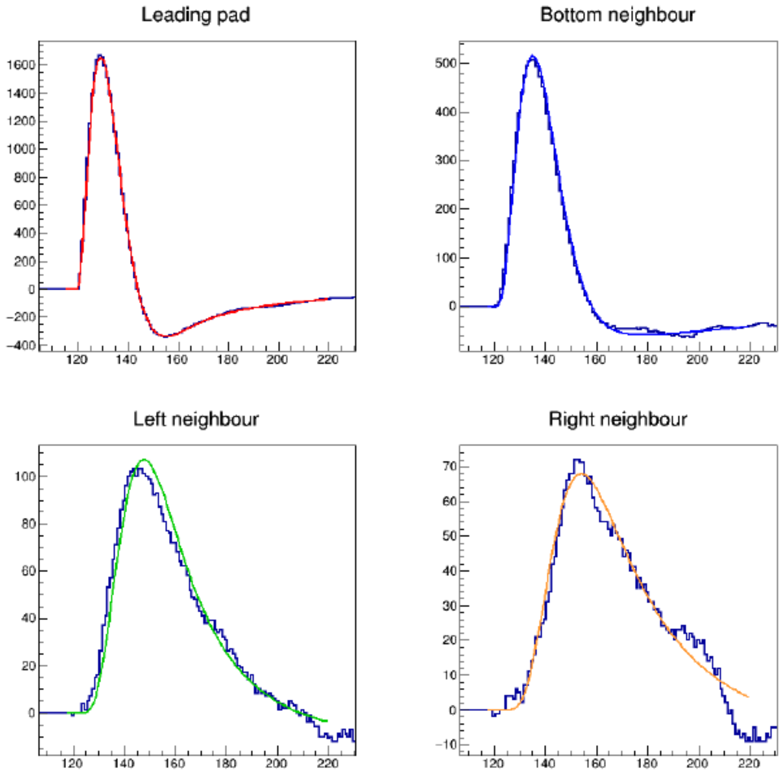

# Summary

- ND280 upgrade employs resistive Micromegas for the read-out of HA-TPC, which works on the principle of charge spreading → 37 have been fully validated.

- Charge spreading model is obtained from convolution of charge diffusion function and electronics response function. The model is able to successfully fit waveforms from X-ray data.
  - RC and Gain are simultaneously extracted from X-ray data.
  - The RC and gain maps uniformity are studied in detail.
  - An energy resolution of about 10% was measured.

- Noise model was built. The nearly identical noise levels across all ERAMs reflect the uniformity of the electronics and the precise mechanical definition of the glue layer, which governs the detector capacitance.

- Results presented in this talk are published in *Nucl.Instrum.Meth.A 1056 (2023) 168534, e-Print: 2303.04481* and coming publications.